Toward a Deterministic Model of Planetary Formation IV:

Effects of Type-I Migration

S. Ida

Tokyo Institute of Technology, Ookayama, Meguro-ku, Tokyo 152-8551, Japan

ida@geo.titech.ac.jp

and

D. N. C. Lin

UCO/Lick Observatory, University of California, Santa Cruz, CA 95064, USA

Kavli Institute of Astronomy & Astrophysics, Peking University, Beijing, China

lin@ucolick.org

ABSTRACT

In a further development of a deterministic planet-formation model (Ida & Lin 2004), we consider the effect of type-I migration of protoplanetary embryos due to their tidal interaction with their nascent disks. During the early embedded phase of protostellar disks, although embryos rapidly emerge in regions interior to the ice line, uninhibited type-I migration leads to their efficient self-clearing. But, embryos continue to form from residual planetesimals at increasingly large radii, repeatedly migrate inward, and provide a main channel of heavy element accretion onto their host stars. During the advanced stages of disk evolution (a few Myr), the gas surface density declines to values comparable to or smaller than that of the minimum mass nebula (MMSN) model and type-I migration is no longer an effective disruption mechanism for mars-mass embryos. Over wide ranges of initial disk surface densities and type-I migration efficiency, the surviving population of embryos interior to the ice line has a total mass several times that of the Earth. With this reservoir, there is an adequate inventory of residual embryos to subsequently assemble into rocky planets similar to those around the Sun. But, the onset of efficient gas accretion requires the emergence and retention of cores, more massive than a few $M_\oplus$, prior to the severe depletion of the disk gas. The formation probability of gas giant planets and hence the predicted

mass and semimajor axis distributions of extrasolar gas giants are sensitively determined by the strength of type-I migration. We suggest that the observed fraction of solar-type stars with gas giant planets can be reproduced only if the actual type-I migration time scale is an order of magnitude longer than that deduced from linear theories. We also show that the introduction of such slower type-I migration rate makes simulated planetary mass-period distribution more consistent with observation.

Subject headings: extrasolar planets – planetary systems: formation – solar system: formation

1. Introduction

In the radial velocity survey of nearby stars, more than 200 extrasolar planets with mass M_p comparable to that of Jupiter M_J have been discovered. Current statistics indicates that $\eta_J > 7\%$ of all nearby F, G, and K dwarfs on various search target lists have gas giant planets with semimajor axis < 5AU (e.g., Marcy et al. 2005; Mayor et al. 2005). But the extrapolation of existing data suggests a higher fraction of solar-type stars may have longer-period gas giant planets (Cumming 2004).

In the previous papers of this series (Ida & Lin 2004a,b, 2005, hereafter referred to as papers I, II, and III), we carried out several sets of simulations with a numerical prescription, which is based on the sequential accretion scenario. We used these results to explain the observed mass and orbital distributions of extrasolar planets and to constrain the intrinsic physics of planet formation through detailed comparisons with the observed data.

In these previous investigation, we have taken into account the effect of gas depletion by assuming that the gas surface density Σ_g declines everywhere exponentially over a characteristic timescale $\tau_{\rm dep} \simeq 1$–10 Myr. With an α prescription for the turbulent viscosity, this assumed global evolution of Σ_g can lead to declining accretion rates which are consistent with those observed (Hartmann et al. 1998). The magnitude of $\tau_{\rm dep}$ sets a strong constraint on the gas giant planet building efficiency (e.g., Ida & Lin 2004a).

We have also assumed that the dust surface density (Σ_d) in these disks is preserved from the initial value we have adopted. The dust grains' mass inferred from the mm observation of continuum radiation from protostellar disks (e.g., Beckwith & Sargent 1996) appears to have a wide dispersion centered around the value of the minimum-mass solar nebula (MMSN) model (Hayashi 1981). We adopted a similar distribution for Σ_d centered around that of MMSN. This assumption, though it greatly simplified our treatment, is less well justified. In

the scaling of Σ_d with that of MMSN, we have inherited the assumption that all the heavy elements were locally retained during the epoch of planet formation.

There are two potential avenues for the depletion of heavy elements: hydrodynamic gas drag of small dust grains and type-I migration of cores due to the tidal interaction with their nascent disks. Here, "cores" mean the protoplanetary embryos which formed as a result of runaway/oligarchic growth of accretion of planetesimals (Kokubo & Ida 1998, 2002). These cores are generally not sufficiently massive to initiate runaway gas accretion. Without much additional growth before the disk gas is severely depleted, these cores would become either rocky planets or ice giants.

In the present paper, we consider the dominant processes after the formation of planetary embryos which are hydrodynamically decoupled from disk gas motions. Prior to the phase of rapid gas accretion, these embedded cores and their surrounding gas exchange angular momentum as they engage in tidal interaction (Goldreich & Tremaine 1980; Lin & Papaloizou 1979). Analytic studies suggest that isolated cores lose angular momentum to the disk exterior to their orbits faster than that they gain from the disk interior to their orbits. This torque imbalance leads to a "type-I" migration. From the linear analysis, the characteristic orbital decay time scale of Earth-mass cores at several AU's in a MMNM is much shorter than 1 Myr (Ward 1986; Tanaka et al. 2002). Accordingly, embryos formed well outside the ice line may migrate to the present locations of the Earth and Venus. But, the mostly refractory compositions of the terrestrial planets in the present-day solar system suggest that they probably did not migrate to their present location from regions well beyond the ice line.

Today, there remains considerable uncertainties in the efficiency of this process (see §2.2). Nevertheless, their formation could have been preceded by a much larger population of cores which did migrate into the Sun. In view of this uncertainty, we carry out a parametric study on the decline of the cores' accretion rate associated with a Σ_d reduction due to the type-I migration of cores (see below). This effect has been neglected in our previous papers.

Heavy elements are also depleted from the disks through "type-II" migration. Due to runaway gas accretion onto a core, the growing gas giant planet eventually acquires sufficient mass to open a gap in the disk and lock itself into a "type-II" migration with the viscous evolution of the disk gas (Lin & Papaloizou 1985, 1993). In the context of solar system formation, Lin (1986, 1995) has speculated that, when the solar nebula was massive, several gas giants may have formed, undergone type-II migration, and eventually merged with the Sun. When the disk's Σ_g decreases below that of the MMSN model, the migration has stalled. According to this scenario, Jupiter and Saturn could be the last survivors of several generations of protoplanets (also see Papaloizou and Terquem 2006), although it may not be easy to form terrestrial planets after preceding gas giants have passed through the inner disk

region (Armitage 2003). A resurgence of this migration and survival scenario (Lin et al. 1996) have been stimulated by the observational discoveries of close-in gas giant planets (e.g., Marcy et al. 2005; Mayor et al. 2005). But, a majority of the known extrasolar planets have periods much longer than a few days. We showed in Papers I and II that their observed logarithmic period distribution can be used to infer comparable timescales for giant planets' migration and disk depletion. However, based on the relative abundance between planets with $a < 0.06$ AU and those between 0.2-2AU's from their host stars, we have to assume that up to 90% of the gas giants which migrated to the proximity of their host stars may have perished.

Here, we focus on the repeated clearing due to type-I migration. We suggest that this self-regulated clearing mechanism limits and determines the amount of heavy elements retained by the cores and residual planetesimals (also see discussion on metallicity homogeneity of open clusters in §4.1). It also results in late formation of gas giants and the marginal probability of gas giants' formation through a series of failed attempts.

The scenario we consider here is similar to the hypothesis proposed by Canup & Ward (2006) in the context of satellite formation around Jovian planets. They suggested that the total mass of the surviving satellites is self-regulated by their type-I migration through their nascent circum-planetary disk which is continuously replenished. In the context of planet formation, McNeil et al. (2005) carried out N-body simulations of terrestrial planets' accretion and growth including the effect of type-I migration. They found that it is possible to retain sufficient amount of solid materials (planetesimals and embryos) to assemble Earth-mass planets within a disk lifetime $\sim 10^6$ years provided the type-I migration rate is slightly slower than that predicted by the linear theory. In these simulations, the initial disk mass in terrestrial planet regions is assumed to be 3–4 times of that of MMSN. Based on an analytic approximation for type-I migration, Daisaka et al. (2006) simulated the evolution of Σ_d under various disk conditions. Their results indicate that the depletion region expands outwards, starting from the disk's inner boundary. They also found that in disks with same dust-to-gas ratio, the asymptotic surface density of the retained embryos decreases with the initial value of Σ_d (and Σ_g) because type-I migration is faster in more massive disks.

Here we consider a much large range of initial conditions. With a comprehensive numerical prescription, we consider the possibility of multiple generation of embryo formation. We show that in relatively massive disks although type-I migration is more effective for individual planetesimals and embryos, it does not necessarily lead to more rapid depletion of the residual population. In these disks, migration starts with smaller individual masses but more generations of embryo form and parish before the initial supply of planet-building blocks is severely depleted. Our results indicate that the total retainable mass of heavy elements only

weakly depends on the initial disk mass.

Although type-I migration places a mass limit on the retainable embryos, it does not quench the formation of Earth-like terrestrial planets because they can be assembled from retainable low-mass embryos after the gas is depleted (Daisaka et al. 2006). Gas giant planets, however, must form in gas-rich disks which appears to be depleted on the time scale $\tau_{\rm dep} \sim$ a few Myr. In addition, they must acquire $\sim 10 M_\oplus$ cores prior to the onset of efficient gas accretion. Although they can form rapidly outside the ice lines on massive disks, early generation of such massive cores quickly migrate into their host stars. But, Thommes & Murray (2006) showed that cores formed after the disk gas has been severely depleted may withstand the disruption by the declining type-I migration. In §3 of this paper, we present results which are consistent with that obtained by Thommes & Murray (2006). We also incorporate gas accretion onto cores and the effect of type-II migration and find that under some circumstances, there is adequate residual gas to promote the efficient gas accretion and the formation of gas giant planets. This "late formation" scenario is conceptually consistent with that inferred from the noble gas enrichment in Jupiter (Guillot & Hueso 2006). Based on this model, we are able to reproduce the observed mass-period distribution of the known gas giant planets around solar type stars provided the efficiency of type-I migration is at least an order of magnitude slower than that derived from the linear theory (see §3). Our conclusion is consistent with the studies by **?** who also found that a necessary condition for the formation of Jupiter and Saturn is a 30-times reduction in the type-I migration rate.

In metal-poor disks, the formation of critical mass cores requires a relatively large gas surface density. In these disks, type-I migration is more effective in clearing the cores prior to the onset of gas accretion. Consequently, the formation of gas giant planets is suppressed. Assuming the disks' initial metallicity is identical to that of their host stars, this effect sharpens the dependence of the predicted formation efficiency of gas giants on the stellar metallicity which is well established in the observational data (Fischer & Valenti 2005).

Since type-I and II migrations are the essential processes which determine the properties of emerging planets, we briefly recapitulate, in §2, their basic physical principles. We also incorporate a quantitative prescription of these processes in our existing comprehensive model for planet formation. The model for the new addition, type-I migration and the decrease in planetesimal surface density due to the migration, is explained in detail. In §3, we carry out a systematic study on how cores' migration may affect the formation of terrestrial planets and gas giant planets. We show that type-I migration delays formation of gas giants, and that it leads to the mass and semimajor axis ($M_p - a$) distribution consistent with that of the known gas giants around G dwarfs. We also study dependence of the the distribution on planet formation parameters, metallicity. The introduction of relatively slow type-I migra-

tion results in the metallicity dependence that may be consistent with observation. Finally, we summarize our results and discuss their implications in §4.

2. Planet formation and migration model

In this paper, we simulate the $M_p - a$ distribution of extrasolar planets, taking into account the effects of cores' type-I migration as well as type-II migration. In Papers I-III, we outlined in detail a quantitative prescription which we used to model the evolution of planetesimals, gas accretion onto protoplanetary cores, the termination of gas giant planet growth, and type-II migration. In this section we briefly recapitulate the dependence of both types of migration on the background disk properties.

In this paper, we newly incorporate the effects of type-I migration and examine the impact of type-I migration on the formation of terrestrial planets and the asymptotic properties of emerging gas giant planets. In light of the theoretical uncertainties, we introduce a prescription which captures the main determining factors of type-I migration and enables us to consider a wide range in the magnitude of its efficiency factor. We here consider only the case of $M_* = 1M_\odot$ to focus on the effects of type-I migration around solar-type stars, although we retain the dependences on stellar mass M_* and its luminosity L_*.

Note that inclusion of type-I migration and the minor changes in truncation conditions of growth of gas giants and the disk model that are described below do not change the conclusions that have been derived in previous papers: (i) the existence of "planet desert" (a lack of intermediate mass planets at $\lesssim$ a few AU) in Paper I, (ii) the metallicity dependence (a fraction of stars with giant planets increases with the metallicity) in Paper II, and (iii) the stellar mass dependence (giant planets are much less abundant around lower-mass stars) in Paper III. The results with inclusion of type-I migration corresponding to (i) and (ii) are shown in Figures 5 and 6, respectively. The stellar mass dependence with type-I migration is briefly commented on in §3.2.3 and will be discussed in detail in a separate paper.

2.1. Parameterized disk models

The main objectives of this series of papers is to examine the statistical properties of emerging planets under a variety of disk environments rather than to study individual processes which regulate the disk structure. For computational convenience, we introduced,

in Papers I-III, multiplicative factors (f_d and f_g) to scale Σ_g and Σ_d such that

$$\begin{cases} \Sigma_d &= \Sigma_{d,10}\eta_{\rm ice} f_d (r/10{\rm AU})^{-q_d}, \\ \Sigma_g &= \Sigma_{g,10} f_g (r/10{\rm AU})^{-q_g}, \end{cases} \quad (1)$$

where normalization factors $\Sigma_{d,10} = 0.32{\rm g/cm}^2$ and $\Sigma_{g,10} = 75{\rm g/cm}^2$ correspond to 1.4 times of Σ_g and Σ_d at 10AU of the MMSN model, and the step function $\eta_{\rm ice} = 1$ inside the ice line at $a_{\rm ice}$ (eq. [3]) and 4.2 for $r > a_{\rm ice}$ [the latter can be slightly smaller (~ 3.0) (Pollack et al. 1994)].

We show below that the disk metallicity $[{\rm Fe/H}]_d$ is an important parameter which regulates the survival of protoplanetary cores during their type-I migration. Dependence of disk metallicity is attributed to distribution of $f_{d,0} = f_{g,0} 10^{[{\rm Fe/H}]_d}$. Solar metallicity corresponds to $[{\rm Fe/H}]_d = 0$ and $f_{d,0} = f_{g,0}$. The main advantage of these parameterized disk structure models is that they enable us to efficiently simulate and to examine the dominant dependence of planet formation and dynamical evolution on the disk structure.

In self-consistent treatment of accretion flow, the disk temperature is determined by an equilibrium between the viscous dissipation and heat transport (Shakura & Sunyaev 1973). We neglect the detailed energy balance (Chiang & Goldreich 1997; Garaud & Lin 2007) and adopt the equilibrium temperature distribution in highly optically thin disks prescribed by Hayashi (1981) such that

$$T = 280 \left(\frac{r}{1{\rm AU}}\right)^{-1/2} \left(\frac{L_*}{L_\odot}\right)^{1/4} {\rm K}. \quad (2)$$

In this simple prescription, we set the ice line to be that determined by an equilibrium temperature (eq. [2]) in optically thin disk regions (Hayashi 1981),

$$a_{\rm ice} = 2.7 (L_*/L_\odot)^{1/2} {\rm AU}, \quad (3)$$

where L_* and $L_\odot$ are the stellar and solar luminosity. The magnitude of $a_{\rm ice}$ may be modified by the local viscous dissipation (Lecar et al. 2006) and stellar irradiation (Chiang & Goldreich 1997; Garaud & Lin 2007). These effects do not greatly modify the disk structure during the late evolutionary stages and they will be incorporated in subsequent papers.

2.1.1. Evolution of f_g

The surface density of the gas can be determined by a diffusion equation (Lin & Papaloizou 1985),

$$\frac{\partial \Sigma_g}{\partial t} - \frac{1}{r}\frac{\partial}{\partial r}\left[3r^{1/2}\frac{\partial}{\partial r}(\Sigma_g \nu r^{1/2})\right] = 0. \quad (4)$$

where we neglected the sink terms due to photoevaporation and accretion onto the cores. For computational convenience, we adopt the standard constant-α prescription for viscosity (Shakura & Sunyaev 1973),

$$\nu = \alpha c_s H, \tag{5}$$

where c_s, $H = \sqrt{2}c_s/\Omega_{\rm K}$, and $\Omega_{\rm K}$ are the sound speed, disk scale height, and the Keplerian angular frequency. Although the value of α is not clear, $\alpha \sim 10^{-3}$ may be consistent with the observational data of accretion rates of T Tauri disks (e.g., Hartmann et al. 1998) and the results of MHD simulations (e.g., Sano et al. 2004). We here use $\alpha = 10^{-3}$ as a nominal value.

With the α prescription and eq. (2), $\nu \propto r$ and eq. (4) reduced to a linear partial differential equation for which self-similarity solutions have been presented by Lynden-Bell & Pringle (1974). The numerical solution for disk-evolution equation [*i.e.*, eq. (4) with $\alpha = 10^{-3}$], starting with $\Sigma_g \propto r^{-1.5}$ for $r < r_m$ and an exponential cutoff at $r_m = 10$AU, is illustrated in Figure 1a.

After a brief initial transition, the numerical solution quickly approaches to $\Sigma_g \propto r^{-1}$ with an asymptotic exponential cut-off, which is the self-similar solution obtained by Lynden-Bell & Pringle (1974) for a linear viscosity prescription and by Lin & Bodenheimer (1982) for an α model. As shown in Figure 1b, Σ_g in the region $r < r_m$ decreases as uniformly independent of r. In the self-similar solution, Σ_g at $r < r_m$ decays as $\Sigma_g \propto (t/\tau_{\rm dep} + 1)^{-3/2}$, where

$$\tau_{\rm dep} = \frac{r_m^2}{3\nu(r_m)} \simeq 3 \times 10^6 \left(\frac{\alpha}{10^{-3}}\right)^{-1} \left(\frac{r_m}{100{\rm AU}}\right) \left(\frac{M_*}{M_\odot}\right)^{-1/2} {\rm yrs}. \tag{6}$$

In the above, we used eqs. (2) and (5).

This self-similar nature of the solution is preserved if we assume a spatially uniform exponential depletion of the disk (*i.e.* $\Sigma_g \propto \exp(-t/\tau_{\rm dep})$ with a r-independent $\tau_{\rm dep}$), as in Papers I-III, although in the actual self-similar solution, $\Sigma_g \propto t^{-3/2}$ for $t > t_{\rm dep}$. If the effect of photoevaporation is taken into account, Σ_g decays rapidly after it is significantly depleted, so that the exponential decay could be more appropriate. Thus, we adopt

$$f_g = f_{g,0} \exp(-t/\tau_{\rm dep}), \tag{7}$$

in the disk model in eq. (1). Even if we fix the α value, $\tau_{\rm dep}$ has uncertainty, because we do not have enough knowledge about r_m, and r_m should have some dispersion. We use $\tau_{\rm dep}$ as a parameter and set it to be in a range of 10^6–10^7 yrs, which may be consistent with observation. Corresponding to the self-similar solution, we consider here disk models with $\Sigma_g \propto r^{-1}$ ($q_g = 1$) in addition to the case with $\Sigma_g \propto r^{-3/2}$ ($q_g = 3/2$) that was assumed in Papers I-III corresponding to the MMSN model.

2.1.2. Evolution of f_d

We start each model with $\Sigma_d \propto r^{-3/2}$ ($q_d = 3/2$). In principle, the evolution of Σ_d should be treated independently from Σ_g even though small dust particles are thermally and dynamically coupled to the gas. Physically, the magnitude of Σ_d is determined by the grains' growth rate and the planetesimals' retention efficiency. In view of the large uncertainties in these processes, we adopt the radial gradient of conventional MMSN model, $q_d = 3/2$. Different radial gradient between Σ_d and Σ_g could be produced by inward migration of dust grains due to gas drag, which tends to make inner disk more metal-rich while outer disk metal-poor (Stepinski & Valageas 1997; Kornet et al. 2001).

In Papers I-III, f_d was assumed to be constant with time until core mass reaches isolation mass. In the present paper, we take into account planetesimal clearing due to the cores' accretion. Since we also include type-I migration of the cores, f_d at a given location (semimajor axis a) continuously decreases with time as planetesimals are accreted by cores which in term undergo orbital decay. Note that in the present paper, a is identified as r, since we neglect evolution of orbital eccentricities.

The full width of feeding zone of a core is given by (Kokubo & Ida 1998, 2002)

$$\begin{aligned} \Delta a_{\rm c} &= 10 r_{\rm H} \\ &= 10 \left(\frac{2M_{\rm c}}{M_*}\right)^{1/3} a, \end{aligned} \tag{8}$$

where $r_{\rm H}$ is two-body Hill radius. Following Papers I-III, we take into account of the expansion of feeding zones due to collisions among the isolated cores after significant depletion of disk gas (Kominami & Ida 2002; Zhou et al. 2007), although this effect influences the results only slightly (it is important in inner regions in which cores are significantly depleted by type-I migration).

An increase in the cores' mass is uniformly subtracted from the mass in its feeding zone, keeping q_d locally. When the cores migrate out from the feeding zone, the reduction of f_d at the initial location of the cores is stopped. But, the cores can continue to accrete planetesimals along their migration path. In any given system, when a core reaches 0.03AU (occasionally, it can attain sufficient mass to accrete gas and become a gas giant during the course of its migration), a next-generation core is launched at the pre-migration radius with 100 smaller mass. (Since core growth is faster during earlier stage of disk evolution (eq. [9]), the choice of initial mass of the next-generation core does not affect the total core accretion timescale.) Thereafter the growth of the core and the depletion of the planetesimals in its feeding zone resume.

This process repeats until the residual planetesimals are depleted. Along the cores'

migrating paths, they accrete residual planetesimals (until they reach $a < a_{\rm dep,mig}$ given by eq. [27]; see below) but cannot reduce f_d as fast as the cores formed *in situ*. Therefore we neglect the evolution of f_d due to the planetesimal accretion by the migrating cores. The clearing of the residual planetesimal disk by migrating gas giants, is also neglected because it rarely occurs and is unlikely to affect the overall distribution of the emerging terrestrial planets (see §3.2.2). The overall evolution of Σ_d due to core accretion and migration is described in §3.1.

2.2. Core growth and type-I migration

We briefly recapitulate a comprehensive analysis on the growth of planetesimals and cores. Readers can find a systematic derivation of these results and the appropriate references from Paper I. During their growth through cohesive collisions, cores' mass accretion rate (of planetesimals) at any location a and time t is described by (Paper I)

$$dM_{\rm c}/dt = M_{\rm c}/\tau_{\rm c,acc};$$
$$\tau_{\rm c,acc} = 2.2\times10^5\eta_{\rm ice}^{-1}f_d^{-1}f_{\rm g}^{-2/5}10^{(2/5)(3/2-q_g)}\left(\tfrac{a}{1{\rm AU}}\right)^{27/10+(q_d-3/2)+(2/5)(q_g-3/2)}\left(\tfrac{M_*}{M_\odot}\right)^{-1/6}{\rm yrs}, \quad (9)$$

where f_d and f_g change with time. In the derivation of the above expression, we have adopted the mass of the typical field planetesimals to be $m = 10^{20}$g. The numerical factor $10^{(2/5)(3/2-q_g)}$ comes from the fact that we scale surface densities at 10AU in eq. (1).

Based on the results of previous numerical simulations (see references in Paper I), we assume that runaway growth phase is quickly transferred to oligarchic growth phase (Kokubo & Ida 1998). During the oligarchic growth phase, the cores' accretion timescale is dominated by their late-stage growth ($\tau_{\rm c,acc} \propto M_{\rm c}^{1/3}$) so that dependence on their initial mass is negligible. In eq. (9), we adopt $M_{\rm c}(0) = m = 10^{20}$g. When $f_g < 10^{-3}$, we use gas-free accretion rate rather than that in Eq. (9) (Paper I),

$$\tau_{\rm c,acc} = 2\times10^7\eta_{\rm ice}^{-1}f_d^{-1}\left(\frac{a}{1{\rm AU}}\right)^{3+(q_d-3/2)}\left(\frac{M_*}{M_\odot}\right)^{-1/2}{\rm yrs}. \quad (10)$$

In Papers I-III, we artificially terminate the cores' accretion at $M_{\rm c} = M_{\rm c,iso}$, where the isolation mass is given by

$$M_{\rm c,iso} \simeq 0.16\eta_{\rm ice}^{3/2}f_d^{3/2}\left(\frac{a}{1{\rm AU}}\right)^{3/4-(3/2)(q_d-3/2)}\left(\frac{M_*}{M_\odot}\right)^{-1/2}M_\oplus. \quad (11)$$

In the present paper, we do not need to adopt an artificial termination to the core growth because when $M_{\rm c}$ approaches isolation $M_{\rm c,iso}$, in situ core accretion is automatically slowed

down by the reduction of f_d. However, in outer regions, ejection of planetesimals by large protoplanets limits their accretion at $M_{\rm e,sca}$ (scattering limit; Paper I). We take this effect into account by adopting an artificial termination for the cores' accretion of planetesimals when they attain a mass $M_{\rm e,sca} \simeq 1.4 \times 10^3 (a/1{\rm AU})^{-3/2} (M_*/M_\odot) M_\oplus$.

Imbalance in the tidal torques from outer and inner disks causes type-I migration of a core. Through 3D linear calculation, Tanaka et al. (2002) derived the time scale of type-I migration,

$$\begin{aligned} \tau_{\rm mig1} &= \frac{a}{\dot{a}} = \frac{1}{C_1} \frac{1}{2.728+1.082 q_g} \left(\frac{c_s}{a\Omega_{\rm K}} \right)^2 \frac{M_*}{M_p} \frac{M_*}{a^2 \Sigma_g} \Omega_{\rm K}^{-1} \\ &\simeq 5 \times 10^4 \times 10^{(3/2-q_g)} \frac{1}{C_1 f_g} \left(\frac{M_{\rm c}}{M_\oplus} \right)^{-1} \left(\frac{a}{1{\rm AU}} \right)^{q_g} \left(\frac{M_*}{M_\odot} \right)^{3/2} \ {\rm yrs}. \end{aligned} \tag{12}$$

where we used eq. (2) and $q_g = 1$–1.5.

In eq. (12), we introduce an scaling factor C_1 to allow for the retardation of type-I migration due to non-linear effects. In the expression of Tanaka et al. (2002), $C_1 = 1$. Many simulations have been carried out (see e.g., Papaloizou and Terquem 2006) with different numerical methods and resolutions, protoplanetary potentials and orbits, and disk structures. They produced a considerable range of the timescale of type-I migration ($\tau_{\rm mig1}$). Retardation processes for this type-I migration include variation in the surface density and temperature gradient (Masset et al. 2006b), intrinsic turbulence in the disk (Laughlin et al. 2004; Nelson & Papaloizou 2004), self-induced unstable flow (Koller & Li 2004; Li et al. 2005), and non-linear radiative and hydrodynamic feedbacks (Masset et al. 2006a). Under some circumstances, C_1 is reduced to be $\lesssim 0.1$ (Dobbs-Dixon et al. 2007, in preparation). In light of these uncertainties, we adopt C_1 as a parameter and mainly examine the slower migration cases with $C_1 < 1$.

Type-I migration can occur before core mass reaches $M_{\rm c,iso}$. In this case, Σ_d (equivalently, f_d) decreases but does not completely vanish. From the decreased Σ_d, new cores accrete with reduced growth rates and isolation masses. The cycle of core growth, type-I migration, and reduction of Σ_d continues until Σ_d decreases to the levels from which only cores small enough not to migrate (Daisaka et al. 2006). We present a detailed discussion on the self-regulation mechanism in later sections.

Under some conditions, the migrating cores can capture and accumulate planetesimals along their paths (Ward & Hahn 1995; Tanaka & Ida 1999). N-body simulation by Daisaka et al. (2006), however, showed that the trapping of planetesimals by the cores is tentative and it does not significantly reduce their accretion rates. In our simulations, we use the accretion rate for migrating cores that is the same as the rate for non-migrating cores

(eq. [9]). For cores in the systems with $q_g = 1$ and $q_d = 1.5$,

$$\begin{aligned} &dM_{\rm c}/dt = M_{\rm c}/\tau_{\rm c,acc}\ ; \\ &\tau_{\rm c,acc} = 3.5\times10^5\eta_{\rm ice}^{-1}f_d^{-1}f_g^{-2/5}\left(\tfrac{a}{1{\rm AU}}\right)^{5/2}\left(\tfrac{M_*}{M_\odot}\right)^{-1/6}{\rm yrs}, \end{aligned} \tag{13}$$

$$\begin{aligned} &da/dt = a/\tau_{\rm mig1}\ ; \\ &\tau_{\rm mig1} \simeq 1.6\times10^5 C_1^{-1}f_g^{-1}\left(\tfrac{M_{\rm c}}{M_\oplus}\right)^{-1}\left(\tfrac{a}{1{\rm AU}}\right)\left(\tfrac{M_*}{M_\odot}\right)^{3/2}\ {\rm yrs}. \end{aligned} \tag{14}$$

The magnitude of f_d is consistently decreased by the increase in $M_{\rm c}$ (see §3.1). Since the accretion rate is determined by the instantaneous local value of f_d, it limits the mass of the migrating cores in a gaseous medium. Prior to the severe depletion of the disk gas, we quench the cores' accretion of planetesimals at $a < a_{\rm dep,mig}$ (eq. [27]) on the basis that there is an inadequate supply of residual planetesimals in these locations to significantly add to their masses. But, during the gas depletion, we assume f_g decays exponentially. After disk gas is significantly depleted ($f_g \lesssim 10^{-3}$), Eq. (10) is used for $\tau_{\rm c,acc}$. We set also da/dt is set to be zero at disk inner edge (~ 0.03AU).

2.3. Formation of gas giant planets

Prescriptions for formation of gas giant planets are the same as those used in Paper I-III, although the cores' rate of planetesimal accretion is revised from Paper I-III by the incorporation of type-I migration and planetesimal depletion. After the formation of these gas giants, we assume all residual planetesimals in the gap is cleared as consequence of dynamical instabilities. These planetesimals are either accreted by the gas giants or scattered elsewhere (Zhou et al. 2007). We neglect the emergence of second-generation cores close to the orbit of gas giants.

In principle, cores with mass much less than that of the Earth can accrete gas. But, unless the heat released during gas and planetesimal accretion is diffused and radiated away, quasi thermal and hydrodynamic equilibrium would be established to prevent further flow onto the cores. Around low-mass cores, the temperature and density of the envelope are low so that heat cannot be easily redistributed through their envelopes. But as the cores grow through planetesimal bombardment beyond a mass

$$M_{\rm c,hydro} \simeq 10\left(\frac{\dot{M}_{\rm c}}{10^{-6}M_\oplus/{\rm yr}}\right)^{0.25} M_\oplus, \tag{15}$$

both the radiative and convective transport of heat become efficient to allow their envelope to contract dynamically (Ikoma et al. 2000). In the above equation, we neglected the depen-

dence on the opacity in the envelope (see Paper I). In regions where the cores have already attained isolation, their planetesimal-accretion rate $\dot{M}_{\rm c}$ is much diminished (Zhou et al. 2007) and $M_{\rm c,hydro}$ can be comparable to an Earth mass $M_\oplus$. But, gas accretion also releases energy and its rate is still regulated by the efficiency of radiative transfer in the envelope such that

$$\frac{dM_{\rm p}}{dt} \simeq \frac{M_{\rm p}}{\tau_{\rm KH}}, \tag{16}$$

where $M_{\rm p}$ is the planet mass including gas envelope. In Paper I, we approximated the Kelvin-Helmholtz contraction timescale $\tau_{\rm KH}$ of the envelope with

$$\tau_{\rm KH} \simeq 10^{k1} \left(\frac{M_{\rm p}}{M_\oplus}\right)^{-k2} \ {\rm yrs}. \tag{17}$$

In order to take into account the uncertainties associated with planetesimal bombardment, dust sedimentation and opacity in the envelope, we adopt a range of values $k1 = 8$–10 and $k2 = 3$–4 (see Papers I and II). Here we use $k2 = 3$ and treat $k1$ as a parameter.

Gas accretion onto the core is quenched when the disk is depleted either locally or globally. We assume that gas accretion is terminated if either the thermal condition or global depletion condition is satisfied. A (partial) gap is formed when the rate of tidally induced angular momentum exchange by the planet with the disk exceeds that of the disk's intrinsic viscous transport (Lin & Papaloizou 1985) (the viscous condition),

$$M_p > M_{\rm g,vis} \simeq 30 \left(\frac{\alpha}{10^{-3}}\right) \left(\frac{a}{1{\rm AU}}\right)^{1/2} \left(\frac{L_*}{L_\odot}\right)^{1/4} M_\oplus. \tag{18}$$

Planets with $M_p > M_{\rm g,vis}$ have sufficient mass to induce the partial clearing of the disk near their orbit. The tidal torque on either side of the gap becomes sufficiently strong to induce the planets to adjust their positions within the gap. This feedback process leads to a transition from type-I to type-II migration. Therefore, we adopt the viscous condition for the onset of type-II migration. In Papers I-III, we adopted $\alpha = 10^{-4}$ as a nominal value. In order to match the simulated $M_p - a$ distribution to the observed data, eq. (18) was arbitrarily multiplied by a scaling factor $A_\nu = 10$.

The previously adopted value of α is smaller than that inferred from the models of protostellar disk evolution (Hartmann et al. 1998). In this paper, we use $\alpha = 10^{-3}$ without imposing the scaling factor. As a result, the condition for the onset of type-II migration is the same as that in Papers I-III.

A clear gap would be formed and gas accretion would be terminated when the planet's Hill radius becomes larger than disk scale height (Lin & Papaloizou 1985) (the thermal

condition) and it is given by (Paper I)

$$M_p > M_{\rm g,th} \simeq 0.95 \times 10^3 \left(\frac{a}{1{\rm AU}}\right)^{3/4} \left(\frac{L_*}{L_\odot}\right)^{3/8} \left(\frac{M_*}{M_\odot}\right)^{-1/2} M_\oplus. \tag{19}$$

While the thermal condition $r_{\rm H} > 1.5H$ was used in Papers I-III, we here used the condition $r_{\rm H} > 2H$, in order to make clear that the asymptotic mass of gas giants is determined by global depletion of disk gas rather than the local thermal condition in the cases with inclusion of type-I migration in which gas giants are formed in relatively late stages. (It can also reflect the effect of gas flow into the gap mentioned below.)

Some numerical simulations indicate that a residual amount of gas may continue to flow into the gap after both the viscous and thermal conditions are satisfied(D'Angelo et la. 2003; Kley & Dirksen 2006; Tanigawa & Ikoma 2007). However, recent numerical simulations (Dobbs-Dixon et al. 2007) also show that the azimuthal accretion flow from the corotation regions onto the planet is effectively quenched despite a diminishing flux of gas into the gap. Since the thermal condition usually requires larger M_p than the viscous condition ($M_{\rm g,th} > M_{\rm g,vis}$), we adopt it as the criterion for the termination of gas accretion in the determination of the asymptotic mass of gas giant planets. But, we take into a residual amount of gas which may leak through the gap and provide an effective avenue for angular transfer between the inner and outer regions of the disk via the gas giant's corotation resonance (§2.4).

Gas accretion may also be limited by the diminishing amount of residual gas in the entire disk even for planets with $M_{\rm p} < M_{\rm p,th}$. In Papers I-III, we assumed that the maximum available mass is determined simply by $M_{\rm g,noiso} \sim \pi a^2 \Sigma_g$. However, because the global limit plays a more important role when type-I migration is incorporated, we use a more appropriate condition $M_{\rm g,noiso} \sim \int_0^{2a} 2\pi a \Sigma_g da$ (We neglect disk gas inflow from far outer regions). For $q_g = 1$,

$$M_{\rm g,noiso} \simeq 3.5 \times 10^2 f_{\rm g,0} \exp\left(-\frac{t}{\tau_{\rm dep}}\right) \left(\frac{a}{1{\rm AU}}\right)^{1/2} M_\oplus. \tag{20}$$

When $M_{\rm g,noiso}$ diminishes below $M_{\rm p}$ or when $M_{\rm p}$ exceeds $M_{\rm g,th}$, gas accretion is terminated.

2.4. Type-II migration

In our previous analysis in Papers I-III, we adopted a simply analytic prescription for type-II migration: (i) before disk gas mass decays to the value comparable to the planet mass, the planet migrates with (unperturbed) disk accretion and (ii) when disk gas mass is comparable to the planet mass, a fraction ($C_2 \sim 0.1$) of the total (viscous plus advective)

angular momentum flux transported by the disk gas (which is assumed to be independent of the disk radius) is utilized by the planet in its orbital evolution.

If the planet's tidal torque can severely clear a gap in the vicinity of its orbit, Σ_g in inner disk region would decrease faster than that in the outer region. The full torque asymmetry leads to $C_2 \simeq 1$ in case (ii). But, when the truncation condition is marginally satisfied, the disk interior to the planet's orbit have a total mass $\gtrsim M_p$ such that it can effectively replenish the angular momentum lost by planet to the outer disk region. There may also be a leakage of gas through the gap region (D'Angelo et la. 2003) which would suppress the degree of torque asymmetry. The protoplanet's corotation resonance may drive an effective angular momentum transfer across the two disk regions separated by the protoplanet.

Protoplanets are formed in disk regions where the midplane is inactive to magneto-rotational instabilities. It is possible that the modest accretion rate onto the host stars flow through this region via an active layer which is exposed to external ionizing photons and cosmic ray particles (Gammie 1996). Different values of effective α's may contribute to the mass flow through the disk and the planet-disk interaction, especially if there is some leakage across the gap region. All of these possible scenarios can lead to $C_2 \ll 1$.

The uninterrupted replenishment of gas into the corotation region may also maintain a finite vortensity gradient and an unsaturated corotation torque (Masset et al. 2006a) which may reduce the efficiency of type-II migration from disk gas accretion even in case (i) (Crida & Morbidelli 2007). However, the results of another set of 2D numerical hydrodynamic simulations (D'Angelo et al. 2006) essentially reproduces the the 1D simulation (Lin & Papaloizou 1986) in which the contribution from the corotation resonance is neglected.

In order to take into account of these uncertainties, we reduce here the migration rate by a factor C_2 for cases (ii) as in Papers I-III,

$$\begin{aligned} \tau_{\rm mig2,ii} &= \frac{1}{C_2}\frac{(1/2)M_p\Omega_{\rm K}(a)a^2}{3\pi\Sigma_g(r_m)r_m^2\nu_m\Omega_{\rm K}(r_m)} \\ &\simeq 5\times10^5 f_g^{-1}\left(\frac{C_2\alpha}{10^{-4}}\right)^{-1}\left(\frac{M_{\rm p}}{M_{\rm J}}\right)\left(\frac{a}{1{\rm AU}}\right)^{1/2}\left(\frac{M_*}{M_\odot}\right)^{-1/2} {\rm yrs}. \end{aligned} \tag{21}$$

When $\tau_{\rm mig2,ii}$ is shorter than the migration timescale for (i), we use the latter timescale,

$$\begin{aligned} \tau_{\rm mig2,i} &= \mid \frac{a}{\dot a} \mid = \frac{a}{(3/2)\nu/a} \\ &\simeq 0.7\times10^5\left(\frac{\alpha}{10^{-3}}\right)^{-1}\left(\frac{a}{1{\rm AU}}\right)\left(\frac{M_*}{M_\odot}\right)^{-1/2} {\rm yrs}. \end{aligned} \tag{22}$$

Due to more accurate estimations, the numerical factors in $\tau_{\rm mig2,i}$ and $\tau_{\rm mig2,ii}$ slightly differ

from those in Papers I-III for the same values of C_2 and α. However, there are still uncertainties in the formula for $\tau_{\rm mig2,ii}$. Furthermore, it is not easy to theoretically evaluate the value of C_2 as well as α. Hence, we vary the magnitude of C_2 and compare the simulated results with the observed data to obtain a calibration. For $\alpha \sim 10^{-3}$, in the limit that $C_2 \sim 1$, most of gas giants are removed from the regions beyond 1AU, which is inconsistent with observed data of extrasolar planets. As shown in Paper II, in order to reproduce M_p–a distribution of observed extrasolar planets, disk depletion timescale $\tau_{\rm dep}$ must be $\sim \tau_{\rm mig2}$ at a few AU. In the present paper, we mostly adopt $C_2\alpha = 10^{-4}$. For $\alpha \sim 10^{-3}$, it corresponds to $C_2 \sim 1/10$. As a result, $\tau_{\rm mig2,ii}$ we adopt here is almost identical to that used in Papers I-III.

3. Effects of type-I migration

In our previous simulations in Papers I-III, the effect of type-II migration was included but that of type-I migration was neglected. In this section, we investigate the effects of type-I migration on the planets' M_p–a distribution.

3.1. Surface density evolution due to type-I migration

In order to analyze the asymptotic M_p-a distribution from the Monte Carlo simulations, we first present the results on the Σ_d reduction due to type-I migration. The relevant time scale here is a function of C_1, f_g and M_p (eq. [12]). The magnitude of the cores' M_p is a function of f_d, f_g and t.

Since type-I and II migrations involve the tidal interaction of embedded cores with the disk gas, the dynamical clearing of the residual planetesimals is suppressed after the gas is severely depleted (except for outer regions in which ejection by massive embryos can be efficient). Since $t \sim \tau_{\rm dep}$ is a critical stage for the build-up and retention of the cores and the onset of gas accretion onto the cores, we are particularly concerned with the residual Σ_d–distribution at this stage. The asymptotic Σ_d–a distribution is determined by $C_1, f_{g,0}$ and $\tau_{\rm dep}$. In this subsection, we show the simulation results with $f_{g,0} = f_{d,0}$, $q_d = 1.5$ and $q_g = 1.0$ at $t = 0$. The results with other reasonable values of $f_{d,0}/f_{g,0}$, q_d and q_g are qualitatively similar. With these initial conditions, we can compute the emergence of cores during the epoch of gas depletion.

Figure 2a shows Σ_d at $t = 10^5, 10^6$, and 10^7 years (dashed, dotted, and solid lines) with $C_1 = 1$ and $f_{g,0} = 3$. These results correspond to surviving protoplanets at $t \sim \tau_{\rm dep}$ for $\tau_{\rm dep} = 10^5, 10^6$, and 10^7 years, although depletion of f_g on time scales $\tau_{\rm dep}$ is not taken into

account here (in the Monte Carlo simulations in section 3.2, the exponential decay, eq. (7), is considered). We generated 1000 semi major axes with a log-uniform distribution in the range of 0.05–50 AU and simulated the growth and orbital migration of cores there. In these simulations, gas accretion onto cores is neglected in order to clearly see the effects of type-I migration. The dynamical interactions among the cores is also neglected. With N-body simulations, Kominami et al. (2005) showed that the dynamical interactions with other cores and planetesimals do not change the cores' type-I migration speed. The results presented in this panel confirm the finding of N-body simulation by Daisaka et al. (2006). They also show that Σ_d is depleted in an inside-out manner. The clearing of planetesimals, along the paths of previous generations of cores, limits the growth of the migrating cores and the gravitational interactions between them. In order to take into account the effect of dynamical clearing in the Monte Carlo simulations (to be presented in next subsection), we terminate the growth of cores after their semimajor axes have decreased below $a_{\rm dep,mig}$ given by eq. (27).

Figure 2d shows that the total mass of the remaining population of cores is $\sim 0.1 M_\oplus$. For these retained cores, $\tau_{\rm mig1} > 3\tau_{\rm c,acc}$ ($\tau_{\rm c,acc} = \dot{M}_{\rm c}/M_{\rm c}$), where a factor 3 reflects an actual timescale to reach $M_{\rm c}$ because $\tau_{\rm c,acc} \propto M_{\rm c}^{1/3}$. From eqs. (13) and (14), the maximum mass of remaining cores ($M_{\rm c,max}$) is given by

$$M_{\rm c,max} \simeq 0.21 C_1^{-3/4} \left(\frac{f_{g,0}}{3}\right)^{3/10} \left(\frac{\eta_{\rm ice} f_{d,0}}{f_{g,0}}\right)^{3/4} \left(\frac{a}{1{\rm AU}}\right)^{-9/8} \left(\frac{M_*}{M_\odot}\right)^{5/4} M_\oplus. \qquad (23)$$

The above expression with $f_{g,0} = f_{d,0}$ reproduces the result at $\gtrsim a_{\rm dep,mig} \sim 1$AU in Figure 2d as well as the weak dependence of $M_{\rm c,max}$ on $f_{g,0}$ and C_1 (Figures 3d and 4d). In order to further examine the $f_{g,0}$ and C_1 dependences, we carry out a set of models with $f_{g,0} = 30$ ($C_1 = 1$) and $C_1 = 0.1$ ($f_{g,0} = 3$) in Figures 3 and 4. In the former case, the disks is marginally self-gravitating and contain a significant fraction of the central stars' mass. The emergence of relatively massive cores is more sensitively determined by C_1, the inefficiency of type-I migration. A large amount of solid materials in the disk does not efficiently promote the formation of massive cores, because the associated dense gas increases type-I migration speed, as already pointed out by Daisaka et al. (2006).

In the inner regions at $a \lesssim 0.3$AU, the cores' accretion proceeds on very short time scales and they reach their isolation mass near their birth place (Figure 2c). Thereafter, most of these cores migrate into their host stars within 10^5 years. Consequently, the local Σ_d is essentially depleted by the formation and migration of the very first generation cores (panel c). This domain is determined by the condition $M_{\rm c,max} \gtrsim M_{\rm c,iso}$. From eqs. (11) and

(23), this condition implies

$$a \lesssim a_{\rm iso,mig} \simeq 0.45 C_1^{-2/5} \left(\frac{f_{g,0}}{3}\right)^{-2/3} \left(\frac{\eta_{\rm ice} f_{d,0}}{f_{g,0}}\right)^{-2/5} \left(\frac{M_*}{M_\odot}\right)^{14/15} {\rm AU}. \quad (24)$$

This expression approximately reproduces the result in Figure 2 and it accounts for the dependence on C_1 and $f_{g,0}$ (see Figures 3c and 4c). The location of $a_{\rm iso,mig}$ does not vary with the slope of the surface density distribution because both competing processes are determined by local properties of the disk.

In the limit of efficient type-I migration (with $C_1 = 1$), most of the cores undergo orbital decay before they attain their isolation mass in the intermediate regions (for Figures 2, 0.3AU $\lesssim a \lesssim$ 10AU). Consequently a significant fraction of Σ_d remains to promote the formation of subsequent-generation cores. The results of our simulations (Figure 2c) show that many generations of cores may emerge at the same disk location. This repeated formation and self-destruction process is even more efficient in massive disks where $f_{g,0} \gg 1$ (see Figure 3c).

In the inner region, surface density is significantly depleted by the N generations of core formation and disruption where

$$N_{\rm gene,1} \simeq \frac{M_{\rm c,iso}}{M_{\rm c,max}} \simeq 4.1 C_1^{3/4} \left(\frac{f_{g,0}}{3}\right)^{6/5} \left(\frac{\eta_{\rm ice} f_{d,0}}{f_{g,0}}\right)^{3/4} \left(\frac{a}{1{\rm AU}}\right)^{15/8} \left(\frac{M_*}{M_\odot}\right)^{-7/4}. \quad (25)$$

As the planetesimal building blocks become depleted, the cores formed at later epochs have masses smaller than $M_{\rm c,max}$. Therefore the above expression for $N_{\rm gene,1}$ slightly under estimates the number of populations of cores which may emerge.

At large disk radii, the number of generation is limited by disk depletion time. In this region,

$$N_{\rm gene,2} = \frac{t}{\tau_{\rm c,mig}(M_{\rm c,max})} \simeq 3.9 C_1^{1/4} \left(\frac{f_{g,0}}{3}\right)^{13/10} \left(\frac{\eta_{\rm ice} f_{d,0}}{f_{g,0}}\right)^{3/4} \left(\frac{a}{1{\rm AU}}\right)^{-17/8} \left(\frac{t}{10^6 {\rm years}}\right) \left(\frac{M_*}{M_\odot}\right)^{-1/4}. \quad (26)$$

This estimate completely reproduces the results in Figures 2c, 3c, and 4c. The actual number of generation is given by $\min(N_{\rm gene,1}, N_{\rm gene,2})$. Significant depletion of the original inventory of heavy elements occurs in the limit $N_{\rm gene,1} \lesssim N_{\rm gene,2}$, that is, within the location

$$a \lesssim a_{\rm dep,mig} \simeq C_1^{-1/8} \left(\frac{f_{g,0}}{3}\right)^{1/40} \left(\frac{t}{10^6 {\rm years}}\right)^{1/4} \left(\frac{M_*}{M_\odot}\right)^{3/8} {\rm AU}. \quad (27)$$

This boundary of disruption zone is in excellent agreement with the critical location within which Σ_d (equivalently, from f_d) has reduced from its initial values by an order of magnitude.

Note that the dependences of $a_{\rm dep,mig}$ on C_1 and $f_{g,0}$ are very weak. As long as $N_{\rm gene,2} > 1$, the disruption zone is confined to $a \sim (t/10^6{\rm years})^{1/4}$ AU, independent of disk surface density and migration speed C_1 (in the limit of small C_1, $N_{\rm gene,2} < 1$ and $N_{\rm gene,1} < 1$, so that no depletion occurs).

These results indicate that, during the early epoch of disk evolution, cores form and migrate repeatedly to clear out the residual planetesimals. This self-regulated process provides an avenue for the host stars to acquire most of the heavy elements retained by the planetesimals. In large, well-mixed molecular clouds where star clusters form, this self-regulated mechanism would lead to stellar metallicity homogeneity (§4.1). The inner disk region contains cores which have started their type-I migration but not yet reached to the disks' inner edge. The average value of Σ_d at these locations, including the contribution of these migrating cores, is two orders of magnitude smaller than its initial value.

Eventually, the disk gas is so severely depleted that relatively massive cores no longer undergo significant amount of type-I migration. As any given disk radius, the condition for retaining 90% of the initial solid surface density is $N_{\rm gene,2} \simeq 0.1 N_{\rm gene,1}$. We find, from eqs. (25), (26), and (27), that this condition is satisfied in regions with

$$a \gtrsim a_{\rm surv,mig} = 10^{1/4} a_{\rm dep,mig} \simeq 2 a_{\rm dep,mig}. \tag{28}$$

Type-I migration leads to a transition in the Σ_d distribution at this orbital radius.

Inside the ice line, type-I migration limits the mass of individual surviving cores. But these cores can coalesce through giant impacts during and after the severe depletion of the disk gas (Kominami & Ida 2002; Ida & Lin 2004a). Provided the total mass of residual planetesimals and cores is $\sim O(1) M_\oplus$ at 1AU $\lesssim a \lesssim$ a few AU, Earth-mass terrestrial planets may form near 1AU. Previous simulations (Chambers & Wetherill 1998; Agnor et al. 1999; Kominami & Ida 2002; Raymond et al. 2004) show that the most massive terrestrial planets tend to form in inner regions of the computational domain where the isolated cores are initially placed. In these simulations, strong gravitational scattering process can inject planetesimals close to the host stars to form smaller planets with relatively close-in orbits.

In general, type-I migration leads to clearing of planetesimals close to their host stars and sets the inner edge of the cores' population at $\sim$ 1AU. The lack of planets inside the Mercury's orbit in our Solar system might also be attributed to this result (Daisaka et al. 2006). In addition, the self-regulated clearing process also leads to $f_d \sim O(1)$ near 1AU for wide variety of initial conditions ($f_{d,0}$). This residual distribution of heavy elements at $\tau_{\rm dep}$ ensures the formation of Mars to Earth-sized terrestrial planets in habitable zones (see §3.2). Even in the limit that the disks' initial Σ_d distribution is much larger than that of MMSN, the reduction of Σ_d at $\lesssim$ a few AU inhibits *in situ* formation of gas giants interior to the ice

line. In contrast to the results in Papers I-III, the inclusion of type-I migration suppresses the rapid and prolific formation of hot Jupiter which in term facilitates the formation and retention probability of habitable terrestrial planets.

We also simulated several models with $q_d = 2$ which correspond to a steeply declining initial surface density distribution. Such a steep gradient of Σ_d could be produced by the inward migration of dust due to the hydrodynamic drag on them by the disk gas (Stepinski & Valageas 1997; Kornet et al. 2001). In this model, a significant amount of solid mass is contained in inner disk regions where cores quickly form and undergo type-I migration. Nearly all the initial mass of solid components in disks is accreted by the host stars through the self-regulation by type-I migration. The results of this model is consistent with the discovery of metallicity homogeneity among the stars in young open clusters (see §4.1).

The above discussions indicate that the formation of Mars to Earth-sized habitable planets depends only weakly on type-I migration speed. However, it is critical for the formation of cores of gas giant planets, because $M_{\rm c,max} \propto C_1^{-3/4}$ (eq. [23]). For giant planets to actually form, sufficiently massive cores must be able to accrete gas on time scales at least shorter than a few folding time of $\tau_{\rm dep}$. For $\tau_{\rm dep} \sim 10^6$–10^7 years, we deduce, from eq. (16) with $k1 = 9$ and $k2 = 3$, that gas giant formation is possible only for $M_{\rm c} \gtrsim$ a few $M_\oplus$. But, type-I migration suppresses the emergence of such massive cores in disk regions with relatively large Σ_g. The results with $C_1 = 1$ in Figures 2d and 3d show that the asymptotic core masses are generally much smaller than that needed to launch efficient gas accretion even though there is little decline in the magnitude of Σ_d.

In the case of $C_1 = 0.1$ (Figure 4d), the cores formed at a few AU originally have $\sim M_\oplus$. Provided the planetesimals along their migration path are not captured onto their mean motion resonances, these cores can grow up to a few $M_\oplus$ through accretion during migration. The core mass is marginal for rapid gas accretion. As shown in eq. (23), in metal-rich disk regions (where $f_{d,0}/f_{g,0} > 1$), more massive cores can be retained with the same amount of solid materials. In this expression, the effects of gas depletion has not been taken into account. But, this process is included in the numerical simulations in §3.2 and it also enhances the mass of retainable cores, especially those which emerge during the advanced stages of gas depletion. These results suggest that gas giants can be formed for $C_1 \lesssim 0.1$. (Alibert et al. (2005) derived a similar condition for formation of Jupiter and Saturn.) In the next subsection, we will show that $C_1 \lesssim 0.1$ reproduces mass and semi major axis distribution of extrasolar gas giants comparable to those observed.

3.2. Mass - semimajor axis distributions

3.2.1. Dependence on type-I migration speed

We now consider the signature of type-I migration on the $M_p - a$ distribution for a population of emerging planets. In the Monte Carlo simulations, we first generate a 1,000 set of disks with various $f_{d,0}$ (the initial value of f_d) and $\tau_{\rm dep}$. We adopt the same prescriptions for the distributions of $f_{d,0}$ and $f_{g,0}$ as those in Paper II. For the gaseous component, we assume $f_{g,0}$ has a log normal distribution which is centered on the value of $f_{g,0} = 1$ with a dispersion of 1 ($\delta \log_{10} f_{g,0} = 1.0$) and upper cut-off at $f_{g,0} = 30$, independent of the stellar metallicity. For the heavy elements, we choose $f_{d,0} = 10^{[{\rm Fe/H}]_d} f_{g,0}$, where $[{\rm Fe/H}]_d$ is metallicity of the disk. We assume these disks have the same metallicity as their host stars.

Following our previous papers, we also assume $\tau_{\rm dep}$ has uniform log distributions in the ranges of 10^6–10^7 yrs. For each disk, 15 a's of the protoplanetary seeds are selected from a uniform log distribution in the ranges of 0.05–50AU, assuming that averaged orbital separation between planets is 0.2 in log scale (the averaged ratio of semimajor axes of adjacent planets is $\simeq 1.6$). This procedure is the same as that adopted in Paper II. Constant spacing in the log corresponds to the spacing between the cores is proportional to a, which is the simplest choice and a natural outcome of dynamical isolation at the end of the oligarchic growth. The log constant spacing for planets and cores with similar masses also maximizes dynamical stability. In the present paper, we neglect dynamical interaction between planets (this issue will be addressed in future papers) and the growth of individual planets are integrated independently. Although the choice of averaged orbital separation is arbitrarily, it would not change overall results with regard to the effects of type-I migration.

In all the simulations presented here, $\alpha = 10^{-3}$ and $M_* = 1 M_\odot$ are assumed. Since the on-going radial velocity surveys are focusing on relatively metal-rich stars, we present the results with [Fe/H] = 0.1 in most cases. The dependence on [Fe/H] is shown in Figures 6. In order to directly compare with observations, we determine the fraction of stars with currently detectable planets as η_J. In the determination of η_J, we assume the detection limit is set by the magnitude of radial velocity ($v_r > 10$m/s) and orbital periods ($T_K < 4$ years). According to the following uncertainty, we exclude close-in planets with $a < 0.05$AU in the evaluation of η_J.

We artificially terminate type-I and II migration near disk inner edge at a 2 day period (~ 0.03AU for $M_* = 1 M_\odot$) in a similar way to Papers I-III. We have not specified a survival criterion for the close-in planets because we do not have adequate knowledge about planets' migration and their interaction with their host stars near inner edge of their nascent disks. Hence, we record all the planets which have migrated to the vicinity of their host stars.

In reality, a large fraction of the giant planets migrated to small disk radii may either be consumed (e.g., Sandquist et al. 1998) or tidally disrupted (e.g., Trilling et al. 1998; Gu et al. 2003) by their host stars. Cores that have migrated to inner edge may also coagulate and form super-earths (e.g., Terquem & Papaloizou 2007). We also neglect such core coagulation near inner edge.

In a set of fiducial models, we adopt $M_* = 1M_\odot$, [Fe/H] = 0.1 and $(k1, k2) = (9, 3)$ for the gas giants' growth rate (eq. [17]). The analytic deductions in the previous subsection suggest that relatively massive cores can be retained to form gas giants provided $C_1 \lesssim 0.1$. Figures 5 show the predicted M_p–a distributions for $C_1 = 0$ (panel b), $C_1 = 0.01$ (panel c), $C_1 = 0.03$ (panel d), $C_1 = 0.1$ (panel e), and $C_1 = 0.3$ (panel f). In order to directly compare the theoretical predictions with the observed data, we plot (in panel a) M_p which is a factor of 1.27 times the values of $M_p \sin i$ determined from radial velocity measurements (http://exoplanet.eu/). This correction factor corresponds to the average value $1/\langle \sin i \rangle = 4/\pi$ for a sample of planetary systems with randomly oriented orbital planes. To compare with the theoretical results with $M_* = 1M_\odot$, we plot only the data of planets around stars with $M_* = 0.8$–$1.2M_\odot$ observed by radial velocity surveys.

All results show "planet desert," which is a lack of intermediate-mass ($M_p \sim 10$–$100M_\odot$) planets at $\lesssim$ a few AU. However, formation probability of gas giants dramatically changes with C_1. The fraction of stars with gas giants η_J changes from 22.9% for the model with $C_1 = 0$ to 0.2% for $C_1 = 0.3$ (see Table 1). In the observed data, $\eta_J \sim 5$–8% around [Fe/H]~ 0.1 (Figure 6).

In contrast, the distributions of retained gas giants are similar to each other except for relatively large C_1. The theoretical predictions are also consistent with the observed distribution in panel a. We carry out a KS test for statistical similarity between the simulated models and the observed data for the parameter domain of 0.1AU $< a <$ 2.5 AU and $M_{\rm p} > 100M_\oplus$. This range corresponds to a maximum rectangular region in which planets are detectable by radial surveys with precision $v_r > 10$m/s and duration < 4 years. Since we have not imposed any criterion for determining the survival probability of short-period planets, the predicted population of planets with $a < 0.1$AU are excluded in the quantitative statistical significance test. Except for the model with $C_1 = 0.3$ (panel f), these models are statistically similar to the observed data within a significant level $Q_{\rm KS} \gtrsim 0.3$ for both semimajor axis and mass cumulative distribution functions. In particular, the model with $C_1 = 0.03$ (panel d) shows an excellent agreement with $Q_{\rm KS} = 0.86$ for the mass function.

In models with $C_1 = 0.3$, only the low-mass cores can survive type-I migration. The envelope contraction time scales for these low-mass cores are generally much longer (eq. [17]) than the gas depletion time scales. Consequently, η_J is very small ($< 1\%$) for the simulated

model with $C_1 = 0.3$. Since type-II migration occurs after planets have acquired a mass which is adequate to open up gaps, the close-in planets with $\gtrsim 100 M_\oplus$ are rare for models with $C_1 = 0.3$, in contrast to the models that type-I migration is neglected or sufficiently reduced (panels b to e).

Assuming the survival fraction of close-in planets is independent their M_p, the magnitude of C_1 can be calibrated from the observed mass distribution close-in planets. In Figure 7a, we plot the mass function for all the planets which are halted artificially at $a = 0.03$ AU. In this panel, we neglect any further evolution including both disruption and collisions. We also consider an alternative limit that after the gas depletion, the multiple-generation of cores which migrated to the proximity of any given star are able to merge into a single terrestrial planet with a mass $M_{\rm mer}$ (Fig. 7b). These results suggest the potential findings of many hot earths, including Neptune-mass planets, with either transit or radial velocity surveys.

The above results clearly highlights the competing effect of type-I migration and gas accretion. In these models, we approximate the gas accretion process with $(k1, k2) = (9, 3)$. The early models of proto-gas-giant planet formation (Pollack et al. 1996) yield slower growth rates and they are better fitted with $(k1, k2) = (10, 3.5)$. But, recent revisions (Ikoma et al. 2000; Hubickyj et al. 2005) of these models indicate that the protogas giants' growth rates can be significantly enhanced by the opacity reduction associated with grain growth or boundary conditions at different regions of the disk (Ikoma et al. 2001). The Kelvin-Helmholtz contraction timescale may also be reduced by turbulent heat transport in the outer envelope of the protoplanets. In view of these uncertainties, we also simulated models with $k1 = 8$ and 10, with $k2 = 3$ for all cases. The predicted η_J are listed in Table 1. For models with $C_1 = 0.03$–0.1 in which type-I migration marginally suppresses the formation of gas giants, the magnitude of η_J depends sensitively on the minimum mass for the onset of dynamical gas accretion (which is represented by $k1$). The results in Table 1 indicate that a smaller value of $k1(= 8)$ can lead to a significant increase in η_J because smaller mass cores can initiate the runaway gas accretion within $\tau_{\rm dep} = 10^6$–10^7 years (eq. [17]).

3.2.2. Preservation of terrestrial planets

Although type-I migration is an effective mechanism to suppress the emergence of gas giant planets, earth-mass planets can form at $\sim$ 1AU even in the limit of $C_1 \sim 1$. (But most terrestrial planets with $a \lesssim 0.3$AU would be eliminated by a full-strength type-I migration.) Not all of these planets formed interior to the ice line may be retained. A fraction of these planets may be trapped onto the mean motion resonance of migrating gas giant planets and be forced to migrate with them (Zhou et al. 2005). In the relatively unlikely event of

inefficient eccentricity damping and very fast type-II migration, some of the embryos along the path of the migrating gas giants may also be scattered to large radial distances and form later generation terrestrial planets (Raymond et al. 2006).

The survival of terrestrial planets depends on their post-formation encounter probability with migrating giant planets. In the absence of any type-I migration, this probability is modest. But the inclusion of a small amount of type-I migration significantly reduce the fraction of stars with massive close-in gas giants because the retention of the progenitor cores becomes possible only at the late stages of disk evolution when the magnitude of Σ_g is reduced. With a limited supply of the residual disk gas, the growth of gas giants and their type-II migration are suppressed.

We find that repeated migration of gas giants is less common in models with $C_1 \gtrsim 0.01$ than those with $C_1 = 0$. The low type-II migration probability reduced the need for efficient disruption of largely accumulated close-in planets (see Paper II). It also ensures that most of the terrestrial planets formed in the habitable zones are not removed by the migrating gas giants. Note that type-I migration also inhibits *in situ* formation of gas giants near 1AU (see §3.1). Thus, a small amount of type-I migration facilitates formation and retention of terrestrial planets in habitable zones in extrasolar planetary systems, rather than inhibits them.

3.2.3. Metallicity dependence

We also study the dependence on other parameters, metallicity ([Fe/H]). As fiducial models, we set $C_1 = 0.03$ and $k1 = 9$ to compare the metallicity dependence. The most massive cores which can form and be retained prior to gas depletion have masses $M_{\rm c,max}$ given by eq. (23). Smaller $f_{g,0}$, larger $f_{d,0}$, or smaller C_1 increases $M_{\rm c,max}$ and would enhance formation of gas giants. The models in Figures 5 have already illustrated the dependence on C_1.

In Paper II, we showed that relatively large values of [Fe/H] (or equivalent $f_{d,0}/f_{g,0}$) enhance the growth rates and increase the isolation masses for the cores, for the disks with the same $f_{g,0}$. Fast emergence of massive cores can lead to the rapid onset of gas accretion. Based on that model, we found η_J increases with [Fe/H], and the simulated of η_J dependence on the [Fe/H] is qualitatively consistent with observed data (Fischer & Valenti 2005).

Here we study the effect of type-I migration on the η_J–[Fe/H] correlation. In Figures 5, [Fe/H] = 0.1 is assumed. We carried out similar simulations with various [Fe/H] and the simulated η_J–[Fe/H] relation is plotted in Figure 6). A comparison between the results here

and those in Paper II shows that type-I migration enhances the η_J–[Fe/H] correlation. In metal-poor disks, $f_{d,0}/f_{g,0} < 1$ and η_J is significantly reduced by type-I migration. But in more metal-rich disks, relatively massive cores can be retained before the disk gas is severely depleted. The resultant steep dependence is in a better agreement with the observed data (open circles in the plot) than in the dependence without type-I migration (filled circles with dashed line), although different choice of assumed averaged orbital separation may change η_J slightly.

Formed planetary systems are affected by stellar mass M_* as well as metallicity. The dependence on M_* was studied in Paper III, using a simple model without the effects of type-I migration. In the paper, we predicted that gas giants are much more rare around M type dwarfs than around FGK dwarfs while super-Earths are abundant around M type dwarfs, which is consistent with radial velocity survey and microlensing survey (Beaulieu et al. 2006). Adding the type-I migration to the simple prescription in Paper III, we found that the above conclusions do not change. Around M type dwarfs, super-earths at 1–3AU, which are inferred to be abundant by microlensing survey, survive type-I migration. In a separate paper, we will address the details of the M_* dependence of planetary systems, taking into account the M_* dependences of many physical quantities.

4. Summary and Discussions

In our previous Monte Carlo simulations of planet formation processes (Papers I, II, and III), we neglected the effects of type-I migration. In the present paper, we have investigated its effects on formation of terrestrial planets and cores of gas giants. We found that type-I migration provides a self-clearing mechanism for planetesimals in the terrestrial-planet region. Although the planetesimal disk at $a \lesssim 1$AU is significantly cleared, the total mass of residual planetary embryos at regions within a few AU is comparable to the Earth's mass, almost independent of the disk and migration parameters. Earth-like planets can be assembled in habitable zones after the depletion of the disk gas.

But this self-regulated clearing process does prevent giant planets from forming at $\sim$ 1AU even in very massive disks. In general, the clearing of cores leads to the late formation of gas giants. When the surface density of the disk gas is reduced below that of the MMNM, type-I migration would no longer be able to remove cores which are sufficiently massive to initiate the onset of rapid gas accretion. This late-formation tendency also reduces the fraction of gas giant which undergo extensive type-II migration. Since migrating gas giants capture and clear cores along their migration paths, type-I migration also facilitates the retention of Earth-mass planets in the habitable zones.

In the limit that type-I migration operates with an efficiency comparable to that deduced from the traditional linear torque analysis (*i.e.* with $C_1 = 1$), all cores would be cleared prior to the gas depletion such that gas giant formation would be effectively suppressed. However, the catastrophic peril of type-I migration would be limited by at least a ten-fold reduction in the type-I migration speed ($C_1 \lesssim 0.1$). In this limit, a substantial fraction of the cores may survive and gas giants would form and be retained with an efficiency (η_J) comparable to that observed.

The above discussions indicate that the formation probability of gas giants is delicately balanced by various competing processes. Since these processes have comparable efficiency, the fraction of solar type stars with gas giants appears to be "threshold" quantity. Small variations in the strength of one or more of these effects can strongly modify the detection probability of extrasolar planets. For example, η_J is observed to be a rapidly increasing function of their host stars' metallicity (Fischer & Valenti 2005). Although we were able to reproduce this observed trend in Paper II, the simulations presented here indicate that this effect is enhanced by a small amount of type-I migration because it is more effective in metal-poor disks.

The M_p - a distribution in Figures 5 also show its sensitive dependence on various other model parameters. The most noticeable dependence is the relative frequency between gas and ice giant planets at several AU from their host stars. These distributions also predict a modest population of close-in cores, a fraction of which may survive and be observable as hot earths.

4.1. Metallicity homogeneity of open clusters

In modern paradigm of star formation (Shu et al. 1987), most of the stellar content is processed through protostellar disks. Gas diffusion in these disks is regulated by the process of turbulent transport of angular momentum whereas the flow of heavy elements is determined by orbital evolution of their main carriers, *i.e.* through gas drag of grains and tidal interaction of planetesimals and cores with the gas. In general the accretion rates of these two components are not expected to match with each other. In fact, the formation of gas giant planets around ∼10% of the solar type stars and the common existence of debris disks requires the retention of heavy elements with masses at least comparable to that of the MMSN. Yet, stars in young stellar clusters are chemically homogenous (Wilden et al. 2002; Quillen 2002; Shen et al. 2005). The observationally determined upper limit in the metallicity dispersion (< 0.03–0.04 dex) among the stars in the Pleiades and IC4665 open clusters implies a total residual heavy element mass (including the planets) to be less than

twice that in Solar system planets.

Clues on the resolution of this paradox can be found in the protostellar disks. Recent models of the observed millimeter continuum SED's suggest that some fraction of classical T Tauri disks has dust mass $\gtrsim 10$ times the total heavy-element mass in Solar system (Hartmann et al. 2006). Their host stars would acquire significant metallicity dispersion if a large fraction of the heavy elements in these disks is retained as terrestrial planets and cores while most of their gas components is accreted by the stars. Hence, an efficient process to clear heavy elements is required.

Although, due to gas drag, dust grains can undergo inward migration and be accreted onto their host stars, we here assume that the formation of planetesimals is a more efficient self-clearing process. In active protostellar disks where Σ_g and Σ_d are much larger than those of MMSN, planetesimals quickly grow into cores which undergo rapid type-I migration. Through a series of numerical simulations, we show that most cores formed interior to $a_{\rm dep,mig} \sim 1$ AU are lost before the disk gas is severely depleted. On a larger spatial and time scales, this process is also effective in transporting most of the original heavy elements to their host stars. Provided their progenitor molecule clouds is thoroughly mixed, this self-regulated clearing process would ensure stars in young clusters acquire nearly uniform metallicity.

4.2. Diversity of giant planets around solar-type stars

Among the stars with known gas giants, a large fraction of them show signs of additional planets. This special multiplicity function is associated with the formation of gaps around the first-born gas giants. Beyond the outer edge of the gap, a positive pressure gradient leads the gas to attain a local super Keplerian velocity. Dust particles and planetesimals accumulate in this region and grow into sufficiently massive cores to initiate the formation of additional planets(Bryden et al. 2000). It is also possible that the planet formation is a threshold phenomenon, *i.e.* the conditions needed to form a multiple-planet systems are marginally more stringent than that for the formation of single gas giants.

The simulations presented here consider the formation probability of individual planets. Although the impact of type-I migration on the residual disk and the formation of multiple generation cores have been taken into account, we have neglected the impact of gas giant formation on the residual disks. Nevertheless, this algorithm can be used to qualitatively describe a threshold scenario for the formation of multiple planets.

The total formation timescale of gas giants is $\tau_{\rm form} \sim \tau_{\rm c,acc} + \tau_{\rm KH}$. In comparison with

both type-II migration and the disk depletion timescales, we find that, provided $\tau_{\rm c,acc} < \tau_{\rm mig1}$,

- Solar-system-like giant planets would form, if $\tau_{\rm form} \sim \tau_{\rm dep}$, because gas giants would not have enough time to undergo extensive type-II migration.
- Eccentric giants would form, if $\tau_{\rm form} < \tau_{\rm dep}$ and $\tau_{\rm mig2} > \tau_{\rm form}$. The second condition implies that nearby second-generation gas giants are likely to emerge, either by spontaneously satisfying the formation conditions or due to an induced formation process(Bryden et al. 2000), before they undergo any significant type-II migration. Orbital instability of closely packed multiple-planet systems would excite their eccentricities(Rasio & Ford 1996; Weidenschilling & Marzari 1996; Lin & Ida 1997; Zhou et al. 2007).
- Close-in giants would form if $\tau_{\rm form} < \tau_{\rm dep}$, and $\tau_{\rm mig2} < \tau_{\rm form}$. They undergo type-II migration before neighboring gas giants form.

In the second case, if $\tau_{\rm mig2} < \tau_{\rm dep}$ and orbital instability does not occur on a time scale $\sim \tau_{\rm dep}$, the multiple planets could be locked into mean-motion resonances during migration. According to the above conditions, the regions in which close-in, eccentric, and solar-system-like giant planets are likely to form are schematically plotted in the $f_{d,0}$–a_0 plane (a_0 is the initial semimajor axis) in Figure 8, neglecting type-I migration. Bright gray, dark gray, and modest gray regions correspond to close-in, eccentric, and solar-system-like giants regions, respectively. A more quantitative set of simulations will be presented in a subsequent paper.

ACKNOWLEDGMENTS. We thank for detailed helpful comments by an anonymous referee. This work is supported by NASA (NAGS5-11779, NNG04G-191G, NNG06-GH45G), JPL (1270927), NSF(AST-0507424, PHY99-0794), and JSPS.

REFERENCES

Agnor, C. B., Canup, R. M. & Levison, H. F. 1999, Icarus, 142, 219

Alibert, Ya., Mousis, O., Mordasini, C. & Benz, W. 2005, ApJ, 626, 57

Armitage, P. J., Livio, M., Lubow, S. H., & Pringle, J. E. 2002, MNRAS, 334, 248

Armitage, P. J. 2003, ApJL, 582, 47

Artymowicz, P. 1993, ApJ, 419, 166

Balbus, S. A., & Hawley, J. F., 1991, ApJ, 376, 214

Beaulieu, J.-P. et al. 2006, Nature, 439, 139

Beckwith, S. V. W. & Sargent, A. I., 1996, Nature, 383, 139

Bodenheimer, P., & Pollack, J. B. 1986, Icarus, 67, 391

Boss, A. P. 1997, Science, 276, 1836

Bryden, G., Rozyczka, M., Lin, D.N.C., & Bodenheimer, P. ApJ, 540, 1091

Burkert, A. & Ida, S. 2007, ApJ, 660, 845

Calvet, N., Hartmann, L. & Strom, S. E. 2000, in Protostars and Planets IV, ed. V. Mannings, A. P. Boss and S. S. Russell (Tucson:Univ. of Arizona Press), 377

Canup, R. M. & Ward, W. R. 2006, Nature, 441, 834

Chiang, E. I. & Goldreich, P. 1997, ApJ, 490, 368

Chambers, J. E. & Wetherill, G. W. 1998, Icarus, 136, 304

Crida, A. & Morbidelli, A. 2007, MNRAS, 377, 1324

Cumming, A. 2004, MNRAS, 354, 1165

Daisaka, K. J., Tanaka, H. & Ida, S. 2006, Icarus, 185, 492

D'Angelo, G., Kley, W. & Henning, T. 2003, ApJ, 586, 540

D'Angelo, G., Lubow, S. H. & Bate, M. R. 2006, ApJ, 652, 1698

Dobbs-Dixon, I., Li, S.-L. & Lin, D. N. C. 2007, ApJ, 660, 791

Fischer, D. A. & Valenti, J. A. 2005. ApJ, 622, 1102

Garaud, P. & Lin, D. N. C. 2007, ApJ, 654, 606

Gammie, C.F. 1996, ApJ, 457, 355

Goldreich, P., & Tremaine, S. 1980, ApJ, 241, 425

Gu, P., Lin, D. N. C., & Bodenheimer, P. H. 2003, ApJ, 588, 509

Guillot, T. & Hueso, R. 2006, MNRAS, 367, L47

Hartmann, L., Calvet, N., Gullbring, E., & D'Alessio, P. 1998, ApJ, 495, 385

Hartmann, L., D' Aleesio, P., Calvet, N., & Muzerolle, J. 2006, ApJ, 652, 472

Hayashi, C. 1981, Prog. Theor. Phys. Suppl., 70, 35

Hubickyj, O., Bodenheimer, P., Lissauer, J. J. 2005, Icarus, 179, 415

Ida, S. & Lin, D. N. C. 2004, ApJ, 604, 388 (Paper I)

Ida, S. & Lin, D. N. C. 2004, ApJ, 616, 567 (Paper II)

Ida, S. & Lin, D. N. C. 2005, ApJ, 626, 1045 (Paper III)

Ikoma, M., Nakazawa, K. & Emori, E. 2000, ApJ, 537, 1013

Ikoma, M., Emori, H. & Nakazawa, K. 2001, ApJ, 553, 999

Kley, W. & Dirksen, G. 2006 å, 447, 369

Kokubo, E. & Ida, S. 1998, Icarus, 131, 171

Kokubo, E. & Ida, S. 2002, ApJ, 581, 666

Kominami, J. & Ida, S. 2002, Icarus, 157, 43

Kominami, J., Tanaka, H. & Ida, S. 2005, Icarus, 178, 540

Koller, J., Li, H. 2004, in The Search For Other Worlds. AIP Conf. Proc., 713, pp. 63-66

Kornet, K., Stepinski, T. F., Rozyczka, M. 2001, å, 378, 180

Laughlin, G., Steinacker, A. & Adams, F. C., ApJ, 309, 846

Lecar, M., Podolak, M., Sasselov, D. & Chiang, E. 2006, ApJ, 640, 1115

Li, H. et al. 2005 ApJ, 624, 1003

Lin, D. N. C. 1986, in The solar system: Observations and interpretations. ed. M.G. Kivelson & E. Cliffs (NJ: Prentice-Hall), 28

Lin, D. N. C. 1995, in Molecular Clouds and Star Formation. ed. C. Yuan & J.H. You. Singapore (World Scientific), 261

Lin, D. N. C. & Bodenheimer, P. 1982, ApJ, 262, 768

Lin, D. N. C., Bodenheimer, P. & Richardson, D. 1996, Nature, 380, 606

Lin, D. N. C. & Ida, S. 1997, ApJ

Lin, D. N. C. & Papaloizou, J. C. B. 1985, in Protostars and Planets II, ed. D. C. Black & M. S.Matthew (Tucson: Univ. of Arizona Press), 981

Lin, D. N. C. & Papaloizou, J. C. B. 1979, MNRAS, 188, 191

Lin, D. N. C. & Papaloizou, J. C. B. 1986, ApJ, 309, 846

Lin, D. N. C., & Papaloizou, J. C. B. 1993, in Protostars and Planets III, ed. E. H. Levy and J. I. Lunine (Tucson:Univ. of Arizona Press), 749

Lynden-Bell, D. & Pringle, J. E. 1974, MNRAS, 168, 603

McNeil, D., Duncan, M. & Levison, H. F. 2005, AJ, 130, 2884

Marcy, G. et al. 2005, Prog. Theor. Phys. Suppl., 158, 24

Masset, F. S., D'Angelo, G. & Kley, W., 2006, ApJ, in press

Masset, F. S., Morbidelli, A., Crida, A., Ferreira, J., 2006, ApJ, 642, 478

Mayor, M., Pont, F. & Vidal-Madjar, A. 2005, Prog. Theor. Phys. Suppl., 158, 43

Nelson, R. P. & Papaloizou, J. C. B. 2004, MNRAS, 350, 849

Papaloizou, J. C. B., Terquem, C. 2006, Rep. Prog. Phys., 69, 119

Pollack, J. B., Hollenbach, D., Beckwith, S., Simonelli, D. P., Roush, T., & Fong, W. 1994, ApJ, 421, 615

Pollack, J. B., Hubickyj, O., Bodenheimer, P., Lissauer, J. J., Podolak, M., & Greenzweig, Y. 1996, Icarus, 124, 62

Quillen, A. C. 2002. AJ, 124, 400

Rafikov, R. R. 2003, ApJ, 125, 922

Rasio, F. A. & Ford, E. B. 1996, Science, 274, 954

Raymond, S. N., Quinn, T. & Lunine, J. I. 2004, Icarus, 168, 1

Raymond, S. N., Mandell, A. M. & Sigurdsson, S. 2006, Science, 313, 1413

Sandquist, E., Taam, R. E., Lin, D. N. C. & Burkert, A. 1998, ApJ, 506, L65

Sano, T., Miyama, S. M., Umebayashi, T., & Nakano, T., 2000, ApJ, 543, 486

Sano, T., Inutsuka, S., Turner, N. J. & Stone, J. M. 2004, Prog. Theor. Phys. Suppl., 155, 409

Shen, Z.-X., Jones, B., Lin, D. N. C., Liu, X.-W., Li, S.-L. 2005, ApJ, 635, 608

Shu, F.H., Adams, F.C., & Lizano, S. 1987, ARA&A, 25, 23

Shu, F. H., Johnstone, D., Hollenbach, D. 1993, Icarus, 106, 92

Shakura, N. I. & Sunyaev, R. A. 1973, A&A, 24, 337

Stepinski, T. F. & Valageas, P. 1997, A&A, 319, 1007

Tanaka, H. & Ida, S. 1999, Icarus, 139, 350

Tanaka, H., Takeuchi, T. & Ward, W. 2002, ApJ, 565, 1257

Tanigawa, T. & Ikoma, M. 2007, ApJ, in press

Terquem, C. & Papaloizou, J. C. B. 2007, ApJ, 654, 1110

Thommes, E. & Murray, N. 2006, ApJ, 644, 1214

Trilling, D. E., Benz, W., Guillot, T., Lunine, J. I., Hubbard, W. B. & Burrows, A. 1998, ApJ, 500, 428

Ward, W. 1986, Icarus, 67, 164

———. 1997, Icarus, 126, 261

Ward, W. & Hahn, J. 1995, ApJL, 440, 25

Weidenschilling, S. J. & Marzari, F. 1996, Nature, 384, 619

Wilden, B.S., Jones, B.F. Lin, D.N.C., & Soderblom, D.R. 2002, AJ, 124, 2799

Zhou, J.-L., Aarseth, S. J., Lin, D. N. C. & Nagasawa, M. 2005, ApJL, 631, L85

Zhou, J.-L., Lin, D.N.C., & Sun, Y.S. 2007, ApJ, in press.

Zhou, J.-L. & Lin, D.N.C. 2007, ApJ, in press.

	$C_1 = 0$	$C_1 = 0.01$	$C_1 = 0.03$	$C_1 = 0.1$	$C_1 = 0.3$
$k_2 = 8$	23.7	19.1	15.9	6.7	2.0
$k_2 = 9$	22.9	17.2	12.1	4.3	0.2
$k_2 = 10$	21.3	12.0	7.9	2.3	0.

Table 1: η_J (in percent) for various C_1 and k_1. Other parameters are fixed: metallicity [Fe/H]= 0.1, stellar mass $M_* = 1 M_\odot$.

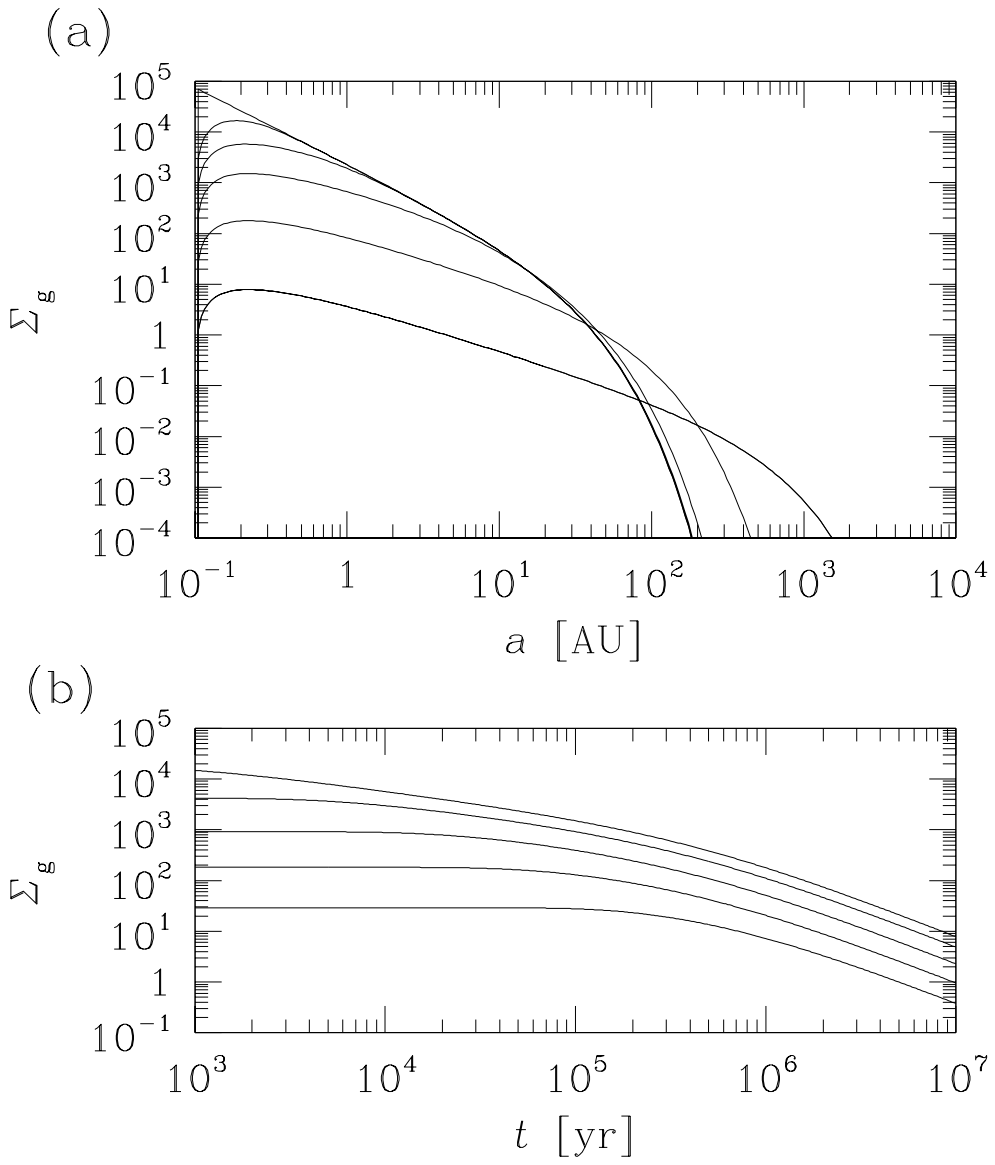

Fig. 1.— Viscous evolution of a disk with $\alpha = 10^{-3}$. We set $\Sigma_g = 0$ at $r = 0.1$AU and 10^5AU. (a) The distributions of Σ_g at $t = 0, 10^3, 10^4, 10^5, 10^6$, and 10^7 years (from top to bottom). (b) Time evolution of Σ_g at planet-forming regions $r = 0.25, 0.67, 1.8, 4.7$, and 12.5 AU (from top to bottom).

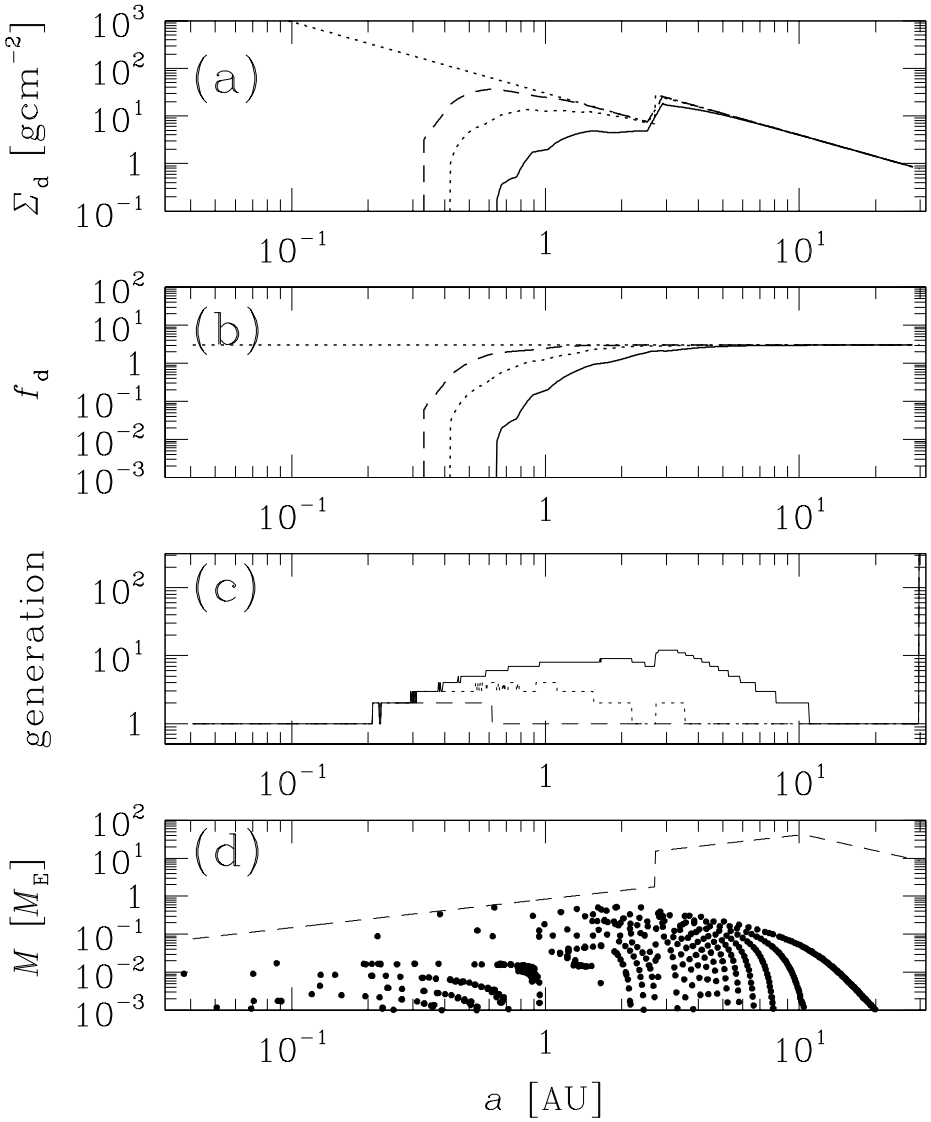

Fig. 2.— The evolution of Σ_d due to dynamical sculpting by type I migration in the case of $C_1 = 1$ and $f_{g,0} = 3$. Here we assume constant f_g. (a) The Σ_d-distributions at $t = 10^5, 10^6$, and 10^7 years are expressed by dashed, dotted, and solid lines. The initial distribution is also shown by dotted lines. (b) The evolution of f_d-distributions. (The meanings of the lines are the same as panel a.) (c) The number of generation of protoplanetary cores formed at each a. (d) Planet distributions at $t = 10^7$ years. The dashed line expresses the core isolation mass and the scattering limit.

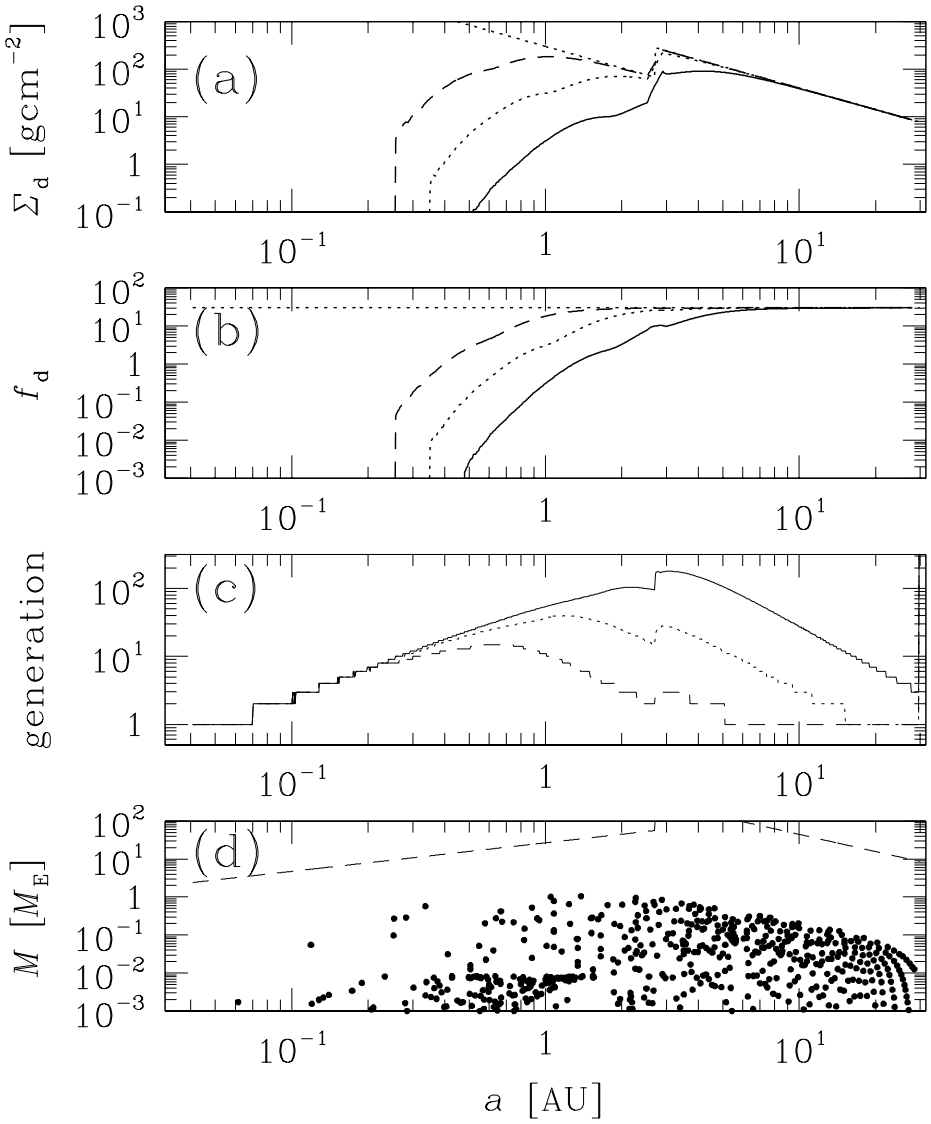

Fig. 3.— The same as Figure 2 except for $f_{g,0} = 30$ to approximate the early phases of massive disk evolution.

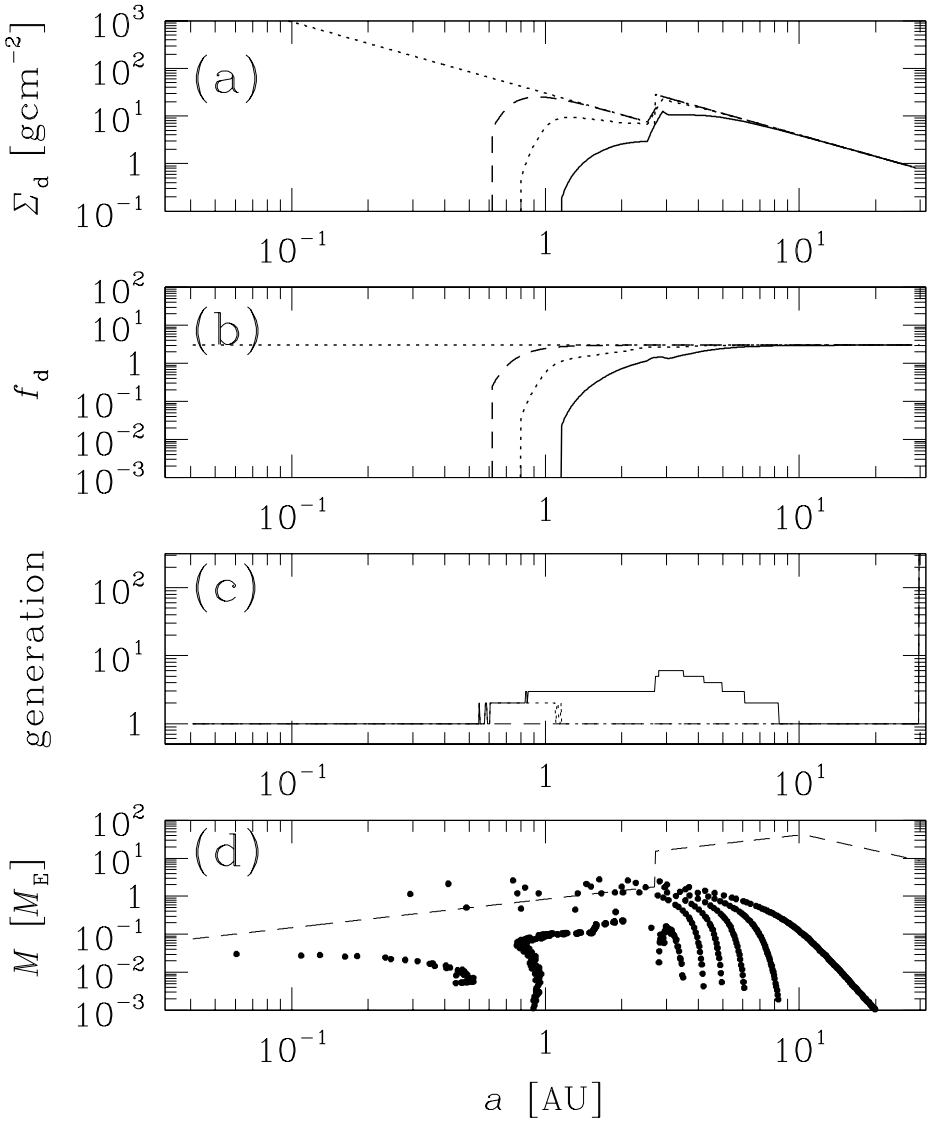

Fig. 4.— The same as Figure 2 except for $C_1 = 0.1$ to approximate weak type I migration.

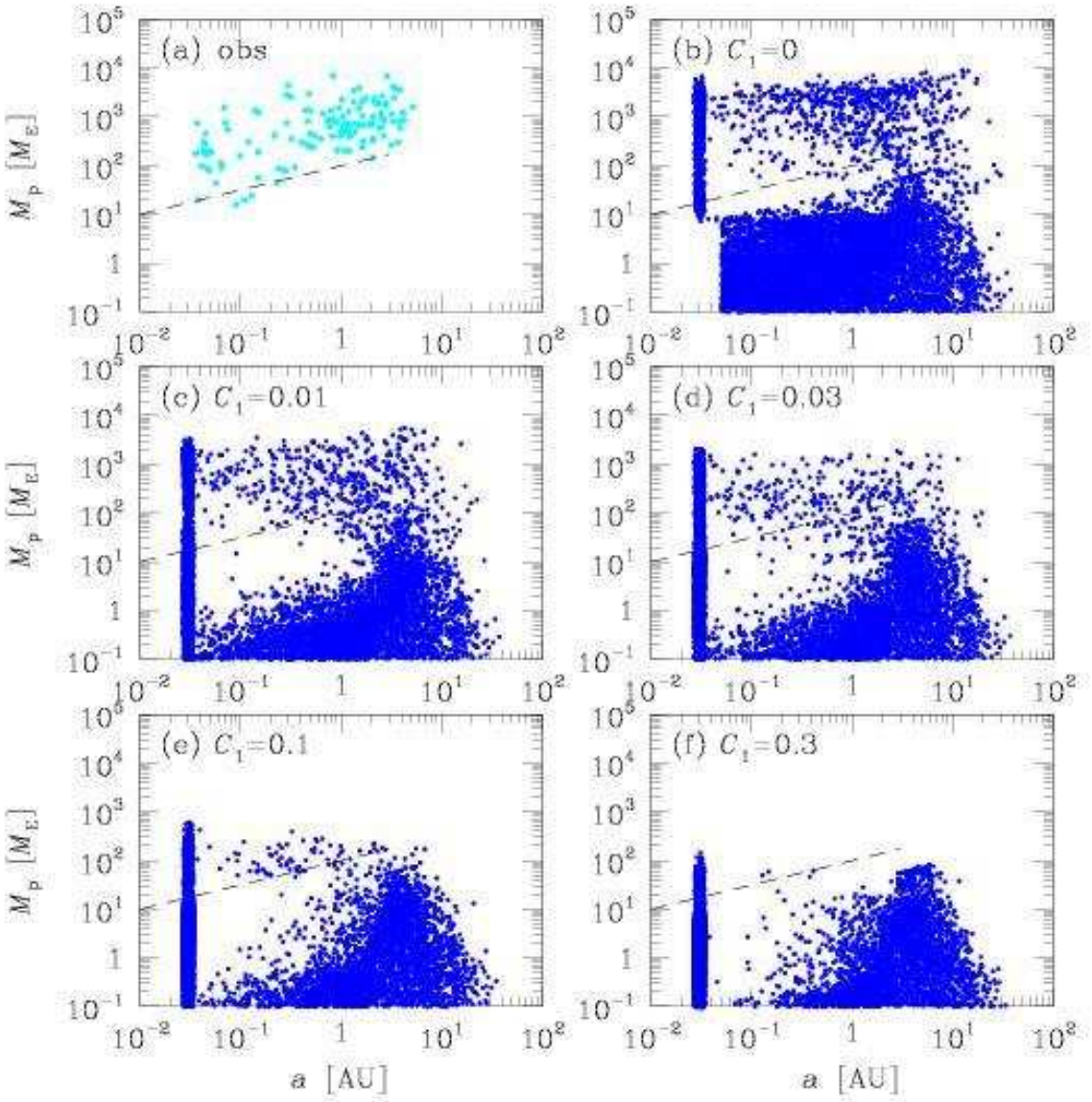

Fig. 5.— Planetary mass and semi major axis distribution. Units of the mass ($M_{\rm p}$) and semimajor axis (a) are earth mass ($M_\oplus = M_{\rm E}$) and AU. (a) Observational data of extrasolar planets (based on data in http://exoplanet.eu/), around stars with $M_* = 0.8$–$1.2 M_\odot$ detected by the radial velocity surveys. The determined $M_p \sin i$ is multiplied by $1/\langle \sin i \rangle = 4/\pi \simeq 1.27$, assuming random orientation of planetary orbital planes. (b) The distribution obtained from Monte Carlo simulations without taking into account the effect of type-I migration, (c) that includes the type-I migration with $C_1 = 0.01$, (d) $C_1 = 0.03$, (e) $C_1 = 0.1$, and (f) $C_1 = 0.3$. The dashed lines express observational limit with radial-velocity measure precision of $v_r = 10$m/s. In these models, $M_* = 1 M_\odot$, the magnitude of the metallicity [Fe/H] $= 0.1$ and the contraction time scale parameters in eq. [17] are assumed to be $(k1, k2) = (9, 3)$.

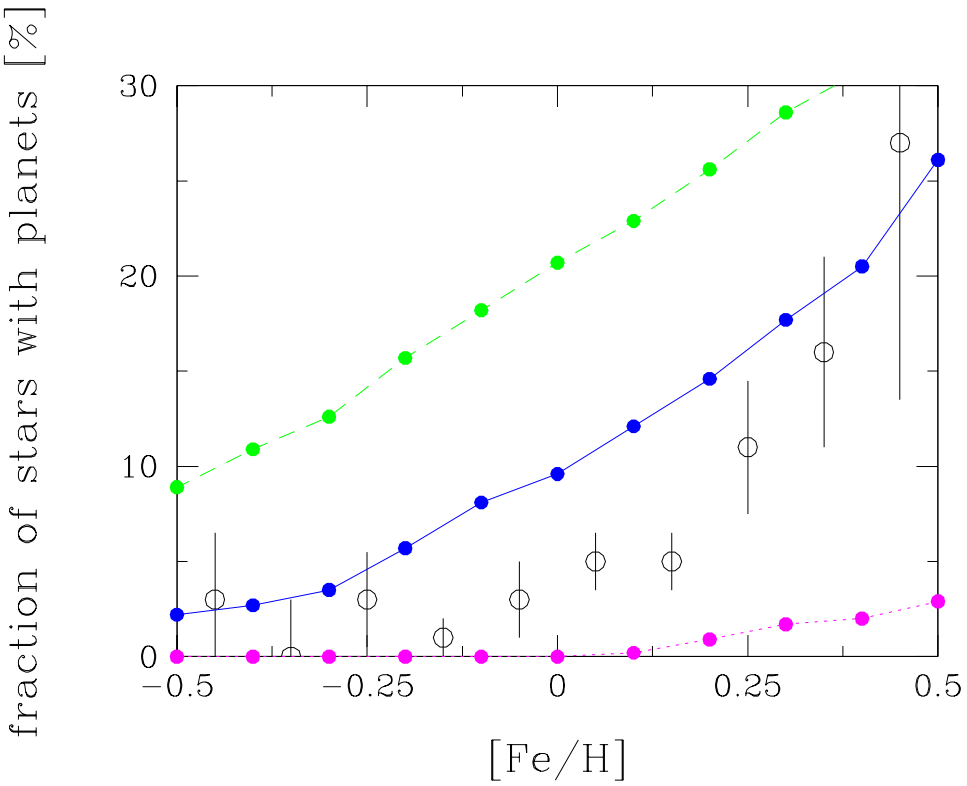

Fig. 6.— The metallicity dependence of fraction of stars with planets which are detectable by radial velocity surveys with measurement precision $v_r > 10$m/s and coverage periods < 4 years. Open circles with error bars are observed data (Fischer & Valenti 2005). Dashed, solid, and dotted lines with filled circles are the theoretically predicted dependences with $C_1 = 0, 0.03$ and 0.3, respectively. Other parameters are $(k1, k2) = (9, 3)$, and $M_* = 1M_\odot$.

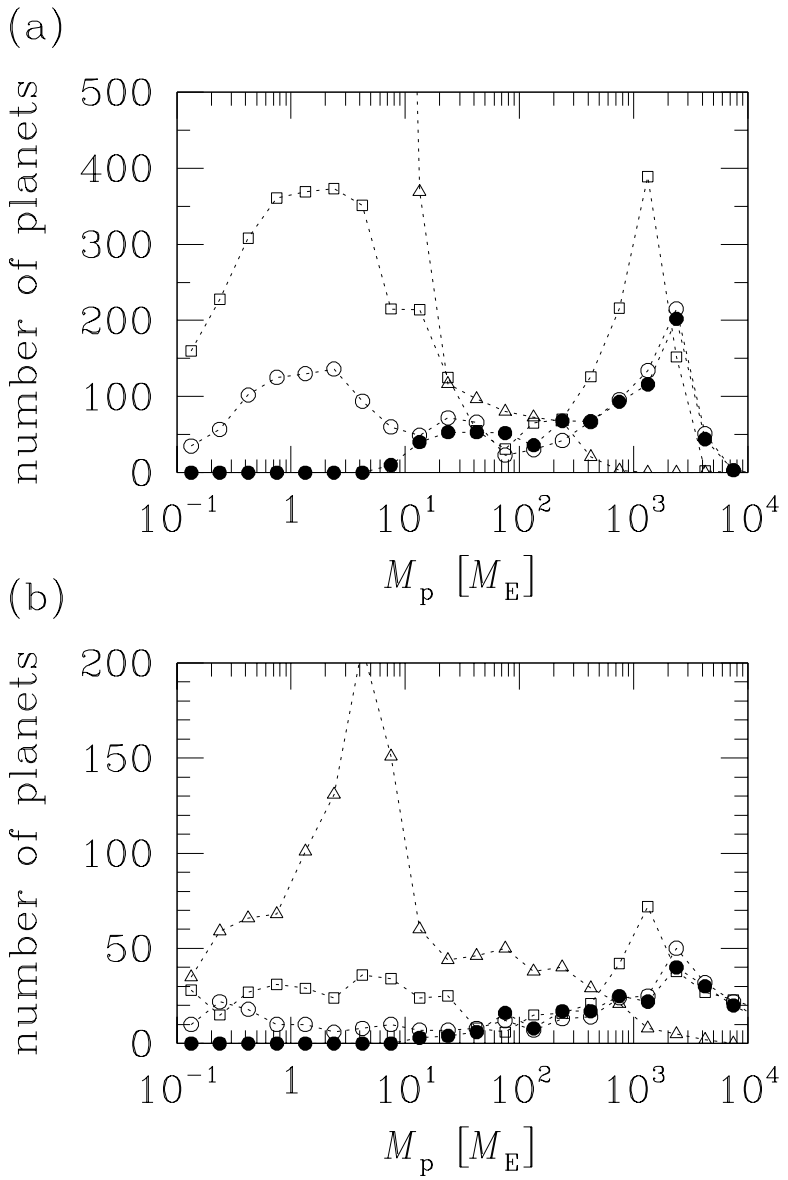

Fig. 7.— The predicted mass function which are halted artificially at $a = 0.03$ AU. (a) The mass function for all the planets, neglecting further evolution due to both disruption and collisions is neglected. Filled circles, open circles, squares, and triangles represent the results with $C_1 = 0, 0.001, 0.01$, and 0.1, respectively. ($M_* = 1M_\odot$, [Fe/H] = 0.1 and $(k1, k2) = (9, 3)$.) (b) That includes the maximum effect of coagulation after the gas is depleted. All the planets are coagulated into one planet in each system.

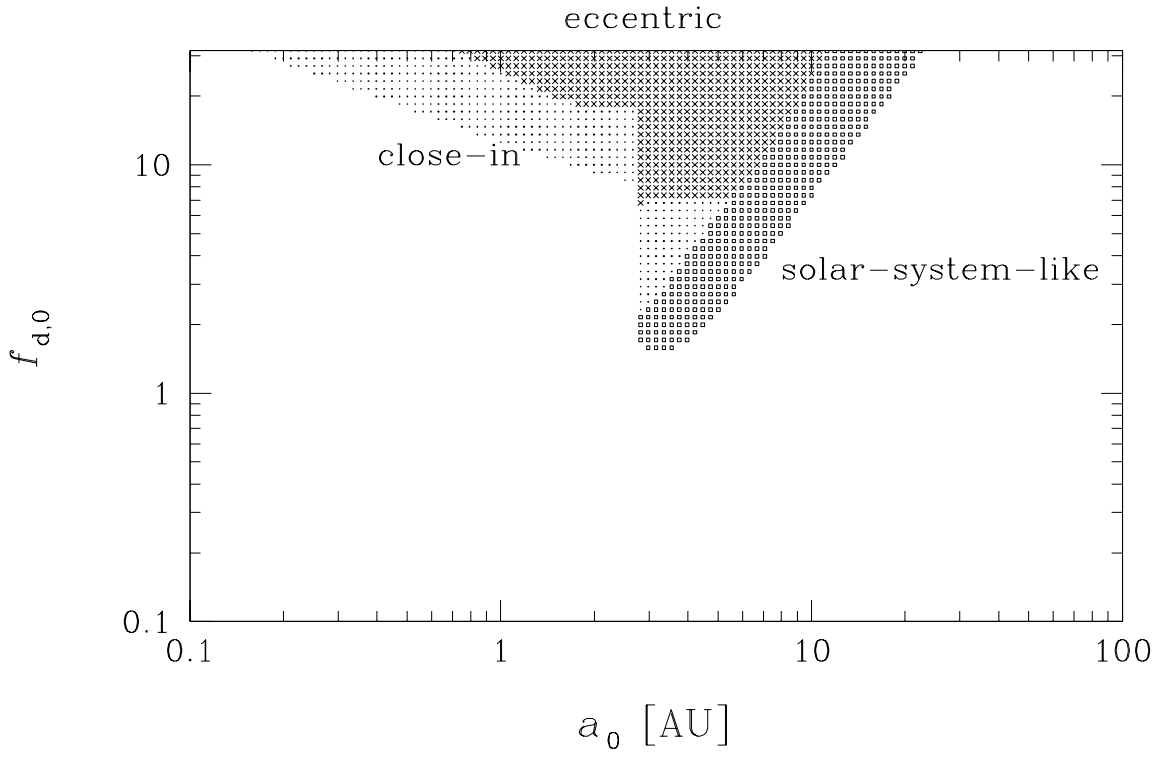

Fig. 8.— The parameter domains (initial disk surface density $f_{d,0}$ and initial semimajor axis of planets a_0), in which close-in, eccentric, and solar-system-like giant planets are likely to form, in the limit of negligible effects of type-I migration. Bright gray, dark gray, and modest gray regions correspond to close-in, eccentric, and solar-system-like giants regions, respectively.